

# **Atmosphere**

**Volume 15 Number 2 1977**

**Canadian Meteorological Society  
Société Météorologique du Canada**

# Atmosphere

Volume 15 Number 2 1977

## Contents

61

Experimental Point and Area Precipitation Probability  
Forecasts for a Forecast Area with  
Significant Local Effects

*Allan H. Murphy and Robert L. Winkler*

79

The Ice Phase and the Evolution of Cloud Droplet Spectra

*H.G. Leighton*

89

On the Breakdown of the Westerlies

*Harald Lejenäs*

114

Notes and Correspondence

115

Book Reviews

116

Call for Papers—Symposium on the Oceanography of the  
St Lawrence Estuary

ISSN 0004-6973

Canadian Meteorological Society  
Société Météorologique du Canada

---

# **Experimental Point and Area Precipitation Probability Forecasts for a Forecast Area with Significant Local Effects<sup>1</sup>**

Allan H. Murphy

*Advanced Study Program, National Center for Atmospheric Research,<sup>2</sup>  
Boulder, Colorado*

and

Robert L. Winkler

*Graduate School of Business, Indiana University, Bloomington, Indiana*

[Manuscript received 27 September 1976; in revised form 10 December 1976]

---

## **ABSTRACT**

This paper describes the results of a recent experiment designed to investigate the ability of forecasters to make point and area precipitation probability forecasts. The location of the experiment (Rapid City, South Dakota) was chosen because of the existence of a network of raingages and because of significant local effects that cause variation among points in terms of precipitation occurrence. A similar experiment conducted at a different location in 1972–73 yielded encouraging results (see Winkler and Murphy, 1976), but the lack of variability in precipitation occurrence among points in the forecast area in that experiment made it difficult to answer several important questions of interest.

On each forecasting occasion during the Rapid City experiment, the forecasters made an average point

probability forecast for the area, individual point probability forecasts for four specific points in the area, an area probability forecast, and an expected areal coverage forecast. The results indicate that the forecasters were able to differentiate with considerable success among the different points in the forecast area in terms of the probability of precipitation. Moreover, the different types of probability forecasts showed a high degree of internal consistency, and the forecasts were all quite reliable and accurate. The results of this experiment, which provide encouraging evidence that forecasters can differentiate among points in such a forecast area and that they can formulate different types of precipitation probability forecasts, have important implications for operational forecasting practices.

---

<sup>1</sup>Supported in part by the National Science Foundation under Grants GA-41232 and ATM74-00161-A01.

<sup>2</sup>The National Center for Atmospheric Research is sponsored by the National Science Foundation.

## **1 Introduction**

Weather forecasters are usually not absolutely certain about the occurrence of future weather events, and probability forecasts enable the forecasters to express their uncertainty in a formal manner. In precipitation forecasting, probability of precipitation (PoP) forecasts provide a quantitative measure of a forecaster's uncertainty concerning the occurrence of precipitation. In this sense, PoP forecasts represent a significant improvement over categorical, or deterministic, forecasts of precipitation (e.g. "rain today") and over forecasts utilizing informal verbal descriptions of the forecaster's uncertainty concerning the occurrence of precipitation (e.g. "a slight chance of rain today"; "rain is likely today"). Specifically, PoP forecasts provide more information than precipitation forecasts not involving probability, and such additional information is valuable to potential users of the forecasts when decisions must be made in the face of uncertainty about the occurrence of precipitation.

A nationwide program involving PoP forecasts was initiated by the U.S. National Weather Service (NWS) in 1965. The official NWS definition of a PoP forecast is an average point probability of measurable precipitation (i.e. at least 0.01 in) for a forecast area. In the forecasts issued by NWS forecasters, the point probability is, in general, assumed to be uniform over the forecast area. Under this assumption, of course, the PoP forecast issued to the public applies to each point in the forecast area. On the other hand, the observation of precipitation is generally taken at only one point, the official raingage.

In many instances, users of precipitation forecasts may be interested in the occurrence of precipitation at points in the forecast area for which the probability of precipitation may be quite different than that at the official raingage. The present practice of issuing an average or uniform point probability for the entire area clearly does not satisfy the requirements of such users unless the point probability is indeed the same at every point in the area. If a forecast area is a very large area, such as an entire state or region of the U.S., then the probability of precipitation obviously will vary from location to location (e.g. from city to city) within the area. The concern in this paper, however, is with variations over a smaller area, such as a single metropolitan forecast area. Local topographic or land-water effects may cause variations in the probability of precipitation over such a forecast area.

When forecasters feel that the point probabilities vary over the forecast area, they occasionally issue two or more forecasts, each of which is applicable to a different portion of the area. The issuance of more than one probability forecast for a forecast area does not appear to be a common practice, however, despite the fact that forecasters in several locations have expressed an interest in making such distinctions more frequently (L.A. Hughes, personal communication). The fact that precipitation is generally observed at only one point, the lack of suitable evidence regarding the forecasters' ability to differentiate among different points, and the extra effort required to make more than one forecast are factors that probably contribute to the reluctance of forecasters to issue different PoP forecasts for different parts of the forecast area.

Another potential difficulty involving PoP forecasts concerns the possibility of misinterpretation of such forecasts. Some members of the public may interpret a precipitation probability in terms of an area probability, an expected areal coverage, or yet some other definition.<sup>3</sup> Moreover, some forecasters may have a definition other than the official definition in mind when making a precipitation probability forecast, as indicated by the responses to a recent questionnaire administered to almost 700 nws forecasters (Murphy and Winkler, 1974). Users, then, are frequently presented with difficult problems related to the interpretation and use of PoP forecasts.

To investigate empirically various types of probability forecasts relating to the occurrence of precipitation, an experiment was conducted at the National Weather Service Forecast Office (wsfo) in St Louis, Missouri, during the period from November 1972 to March 1973. The experiment was designed to investigate the ability of forecasters to differentiate among points in a forecast area with regard to the likelihood of the occurrence of measurable precipitation and the relative ability of forecasters to make point and area (including areal coverage) precipitation probability forecasts. Detailed results of the St Louis experiment are presented in Winkler and Murphy (1976). Evaluations of average point probability forecasts, individual point probability forecasts, and expected areal coverage forecasts revealed that these forecasts were quite reliable and accurate and that they were also internally consistent in the sense that the relationships among these forecasts satisfied the conditions required for consistency in terms of probability theory. On the other hand, the area probability forecasts tended to be too low and were inconsistent with the other forecasts. With regard to point-to-point differences, the forecasters did not differentiate among the points very often, but the absence of such differences seems to have been justified by the lack of variability exhibited by the observations of precipitation occurrence.

An important consideration in the selection of the St Louis wsfo for the initial experiment involving point and area precipitation probability forecasts was the existence of a reasonably dense network of recording raingages in the St Louis metropolitan area. Without such a network, it would have been impossible to evaluate the different types of precipitation probability forecasts except in terms of internal consistency. Nevertheless, to investigate the ability of forecasters to differentiate among points in the forecast area, some variability among the points is obviously desirable. In this regard, the lack of variability among points during the St Louis experiment may have been due to the fact that the St Louis area is not subject to any pronounced local effects (such as a topographic effect) or to the fact that the experiment was conducted in the winter, which tended to minimize the effects of mesoscale weather systems. Thus, although the St Louis experiment indicated that forecasters can make

<sup>3</sup>It should be mentioned that while some members of the public do not fully understand the concept of probability, the primary source of misinterpretation of PoP forecasts is the definition of the precipitation event (e.g. precipitation in an area versus precipitation at a point).

various types of precipitation probability forecasts with some success (all forecasts except the area probability forecasts were quite reliable and accurate), this result might not generalize to situations in which more variability exists among points. Moreover, questions regarding the ability of forecasters to differentiate among points were largely unanswered by the results of the St Louis experiment.

In order to further investigate the questions that motivated the St Louis experiment, a second experiment was recently conducted at the National Weather Service Office (wso) in Rapid City, South Dakota. Rapid City was chosen because of the existence of a network of raingages and because of significant local effects (in particular, the Black Hills) that are known to cause variation among points in terms of precipitation occurrence. The experiment was conducted in the summer in order to further increase the likelihood of such point-to-point variation.

The design of the Rapid City experiment is described in Section 2, and the results of the experiment are presented in Section 3. Section 4 contains a brief summary of the Rapid City experiment, including a comparison of the Rapid City results with the St Louis results, and a brief discussion of the implications of these experiments for future work in the area and for the practice of precipitation probability forecasting.

## **2 Design of the Rapid City experiment**

The subjects in the experiment were nine weather forecasters from the Rapid City wso. Each time the forecasters were on public weather forecasting duty during the period of the experiment, they made point and area precipitation probability forecasts for the Rapid City area. In particular, the forecasters were asked for (i) an average point probability of measurable precipitation for the entire forecast area; (ii) point probabilities of measurable precipitation at four specific points (raingages) in the forecast area; (iii) an area probability of measurable precipitation for the forecast area; and (iv) the expected areal coverage of the forecast area by measurable precipitation.

For the purposes of this experiment, the forecast area was defined by ten points corresponding to recording raingages in the Rapid City area. These raingages were operated by the nws (3 gages), the South Dakota School of Mines and Technology (5 gages), and the United States Forest Service (2 gages). Within the constraints imposed by the location of available raingages, the ten points were chosen in such a way as to obtain a "representative" coverage of the Rapid City area, while including some variation in terms of topography. A map of the area on which the locations of the ten gages have been indicated is presented in Fig. 1.

The four points for which individual point probabilities were assigned corresponded to raingages 1 (airport), 2 (city), 3 (Brownsville), and 4 (Hill City) in Fig. 1. Note that gages 1 and 2 are in or east of Rapid City, while gages 3 and 4 are in the Black Hills west of the city. The average point probability provided by the forecasters was an average point probability for the entire area, not just

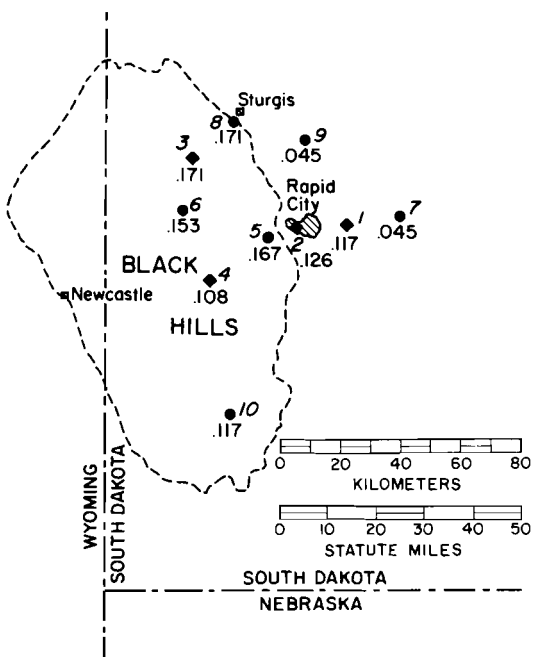


Fig. 1 Network of ten raingages defining the forecast area in the Rapid City experiment. Raingages 1–4 correspond to the locations for which individual point probability forecasts were made (1 – airport, 2 – city, 3 – Brownsville, and 4 – Hill City). The relative frequency of measurable precipitation during the experimental period is indicated for each raingage.

an average point probability for the four points for which individual point probabilities were obtained. The area probability was specifically defined as the probability of measurable precipitation at one or more of the ten points constituting the forecast area, and the expected areal coverage was defined as the expected proportion of the ten points at which measurable precipitation would be observed, given that precipitation occurred at one or more of the points.<sup>4</sup>

Prior to the start of the experiment, the forecasters were given instruction sheets that included precise definitions of the different probabilities and of the forecast area and an explanation of the procedural details of the experiment. The definitions of the probabilities were also included on the forecast sheets in a further attempt to avoid any confusion on the forecasters' part. The forecasters were instructed to make their forecasts at approximately 0400 on the midnight shift and 1600 on the day shift. On each forecasting occasion, the forecasts were made for the next twelve-hour period.<sup>5</sup> The numbers that could

<sup>4</sup>The expected areal coverage, then, is conditional upon the occurrence of precipitation in the area. This *conditional* expected areal coverage should be carefully distinguished from an *unconditional* expected areal coverage. The latter includes situations in which the areal coverage is zero, whereas the former ignores such situations.

<sup>5</sup>In this paper, "day-period forecasts" and "night-period forecasts" refer to forecasts

be used for the point and area probability forecasts were 0.00, 0.02, 0.05, 0.10, 0.20, 0.30, ..., 0.90, and 1.00, while the numbers that could be used for the expected areal coverage forecasts were limited to 0.00, 0.10, 0.20, ..., 0.90, and 1.00.

The Rapid City experiment covered a period from June through September 1974. During that period, 222 sets of forecasts were obtained, 112 sets for the day period and 110 sets for the night period. The number of sets of forecasts for individual forecasters ranged from 13 to 51, with two of the nine forecasters preparing over 25 sets of forecasts (Forecaster 5, with 51 sets, and Forecaster 7, with 44 sets).

### **3 Results of the Rapid City experiment**

The results of the Rapid City experiment are organized by specific types of forecasts. First, the individual point probabilities are examined and the ability of the forecasters to differentiate among the four points for which individual point probabilities were assigned is investigated. Next, the average point probabilities and the consistency of these probabilities with the individual point probabilities are studied. The third type of forecast to be evaluated is the area probability, and the consistency of area probabilities with individual point probabilities is of interest. Finally, the expected areal coverage forecasts and the consistency of these forecasts with the average point probabilities are examined. The analysis of the experimental data, then, involves the consistency among different types of precipitation probability forecasts as well as the reliability and accuracy of each specific type of forecast.

Unless otherwise stated, all results in this section refer to the entire sample of 222 sets of forecasts. Where appropriate, some results pertaining only to the forecasts valid during the day period, the forecasts valid during the night period, or the forecasts prepared by particular forecasters are presented. In cases for which no systematic differences were found between the day period and the night period or among forecasters, the results are not, in general, presented by period or by forecaster.

#### **a Point Probability Forecasts for Specific Points**

The forecasters participating in the experiment were asked for point probabilities of measurable precipitation at four specific points in the forecast area. These four points corresponded to raingages 1–4 in Fig. 1, and the point probability for gage  $i$  is denoted by  $p_i$ . The averages and standard deviations of  $p_1$ ,  $p_2$ ,  $p_3$ , and  $p_4$  for the entire experiment, for the day-period forecasts, and for the night-period forecasts are presented in Table 1. Note that the average values of the point probabilities for the entire experiment ranged from 0.083 at gage 1 to 0.205 at gage 3. On the average, the forecasters clearly differentiated among the four points. Moreover, the points with higher average prob-

---

*prepared* during the midnight shift and day shift, respectively. Thus, day-period forecasts are prepared early in the morning and apply to 0600–1800, a daytime period; night-period forecasts are prepared late in the afternoon and apply to 1800–0600, a nighttime period.

TABLE 1. Averages (standard deviations) of the probability forecasts and selected functions of the probability forecasts\*

	All forecasts (n = 222)	Day-period forecasts (n = 112)	Night-period forecasts (n = 110)
$p_1$	0.083(0.123)	0.080(0.109)	0.086(0.136)
$p_2$	0.123(0.162)	0.137(0.162)	0.108(0.161)
$p_3$	0.205(0.202)	0.250(0.214)	0.159(0.179)
$p_4$	0.172(0.176)	0.189(0.174)	0.154(0.177)
$\bar{p}_f$	0.119(0.151)	0.132(0.150)	0.106(0.152)
$\bar{p}_c$	0.146(0.158)	0.164(0.157)	0.127(0.158)
$m$	0.213(0.207)	0.256(0.213)	0.170(0.192)
$s_p^2$	0.007(0.011)	0.010(0.013)	0.004(0.006)
$a$	0.356(0.305)	0.420(0.311)	0.292(0.285)
$e^\dagger$	0.274(0.167)	0.281(0.162)	0.267(0.173)

\* $p_1, \dots, p_4$  are the four point probabilities;  $\bar{p}_f$  is the forecast average point probability;  $\bar{p}_c$  is the calculated average point probability,  $\sum_i p_i / 4$ ;  $m$  is the largest point probability,  $\max_i \{p_i\}$ ;  $s_p^2$  is the sample variance of the point probabilities,  $\Sigma_i (p_i - \bar{p}_c)^2 / 3$ ;  $a$  is the area probability; and  $e$  is the expected areal coverage.

†The averages and standard deviations of  $e$  were computed only for the periods during which precipitation occurred at one or more of the gages defining the forecast area ( $n$  equals 90 for all, 48 for day period, and 42 for night period).

abilities are located in portions of the forecast area in which topographic features would be expected to increase the frequency of occurrence of precipitation. In particular, higher average probabilities were assigned to gages 3 and 4, which are in the Black Hills west of Rapid City, than to gages 1 and 2, which are in or east of the city itself. In addition, the average probabilities showed considerable variation between the day-period forecasts and the night-period forecasts, with the day-period probabilities being greater, on the average, than the night-period probabilities except at gage 1 (airport). This result is reasonable, suggesting that the forecasters believed that precipitation cells would form over the Black Hills during the afternoon and would generally move eastward at night.

The individual point probabilities, then, showed considerable variation on the average. How much variation did they show within forecast sets? Each forecast set includes four point probabilities, which could all have been assigned the same value (e.g.  $p_i = 0.2$  for  $i = 1, \dots, 4$ ), all assigned different values, or two or three different values could have been used. The percentages of forecast sets with 1, 2, 3, and 4 values for the point probabilities are presented in Table 2, and these percentages indicate a great deal of variation among the point probabilities within forecast sets. The four point probabilities were equal (i.e. only one probability value was used) for only 17.1 per cent of the forecast sets. This result is in marked contrast to that obtained in the St Louis experiment, for which the point probabilities (five instead of four, as in Rapid City) were equal for 80.3 per cent of the forecast sets. With regard to day-period/night-period differences, more variation existed among the point probabilities valid during the day period, as expected. For the day-period (night-period) forecasts, the four gages were assigned four different probability values on

TABLE 2. Percentages of forecast sets containing 1, 2, 3, and 4 values for the four individual point probabilities, and average number of values per forecast set

Forecasts	<i>n</i>	Percentages				Average number of values
		1 value	2 values	3 values	4 values	
All	222	17.1	37.4	32.4	13.1	2.41
Day period	112	12.5	25.0	42.0	20.5	2.71
Night period	110	21.8	50.0	22.7	5.5	2.12

20.5 (5.5) per cent of the forecasting occasions. The average number of values used for the four point probabilities was 2.71 (2.12) for the day (night) period. With regard to individual forecasters, the two forecasters with over 25 sets of forecasts showed greater variability among points than did the other seven forecasters. Forecasters 5 and 7 averaged 2.61 and 2.89 values per set of four point probabilities, respectively, while the remaining forecasters averaged 2.17 values per set.<sup>6</sup>

Another measure of the variability among point probabilities within a forecast set is the sample variance computed from the four probabilities making up the set. This sample variance is  $s_p^2 = \sum_i (p_i - \bar{p}_c)^2 / 3$ , where  $\bar{p}_c = \sum_i p_i / 4$  is the calculated average of the four point probabilities.<sup>7</sup> The average value of  $s_p^2$  was 0.007, as shown in Table 1, and  $s_p^2$  was much higher on the average for the day-period forecasts than for the night-period forecasts. (For the St Louis experiment, the average value of  $s_p^2$  was only 0.001.) The results in Table 2 and the average value of  $s_p^2$  indicate that the individual point probabilities showed considerable variation within forecast sets.

During the experiment, forecasts were made for a total of 222 twelve-hour periods. The corresponding observations for these periods were obtained for the ten raingages defining the forecast area, and the relative frequencies of precipitation at these gages for the 222 periods are presented in Fig. 1 and in Table 3, which also shows the relative frequencies for the twelve-hour intervals covered by the day-period and night-period forecasts. The relative frequencies for the entire experiment ranged from 0.045 to 0.171, and a moderate amount of day-night variation existed. The average absolute difference between the relative frequency corresponding to the day-period forecasts at a particular gage and the relative frequency corresponding to the night-period forecasts at the same gage was 0.033, and the largest such absolute difference was 0.078 at gage 5. With regard to average differences, the day-period relative frequency exceeded the night-period relative frequency by 0.014, although three of the raingages in the four-gage network received precipitation more frequently at night. Thus, on the average, there was a considerable amount of gage-to-gage

<sup>6</sup>It should be noted that Forecasters 5 and 7 made most of their forecasts while on the midnight shift. Thus, differences between these forecasters and the other seven forecasters may be due in part to day-period/night-period differences.

<sup>7</sup>The subscript on  $\bar{p}_c$ , which indicates that it was calculated from the point probabilities, differentiates  $\bar{p}_c$  from  $\bar{p}_f$ , the average point probability formulated by the forecaster.

TABLE 3. Relative frequency of precipitation at individual raingages and in the forecast area

Gage/area	All forecasts (n = 222)	Day-period forecasts (n = 112)	Night-period forecasts (n = 110)
Gage 1	0.117	0.089	0.145
Gage 2	0.126	0.134	0.118
Gage 3	0.171	0.161	0.182
Gage 4	0.108	0.107	0.109
Gage 5	0.167	0.205	0.127
Gage 6	0.153	0.179	0.127
Gage 7	0.045	0.036	0.055
Gage 8	0.171	0.196	0.145
Gage 9	0.045	0.054	0.036
Gage 10	0.117	0.125	0.109
Average for four-gage network	0.131	0.123	0.139
Average for ten-gage network	0.122	0.129	0.115
Area*	0.405	0.429	0.382

\*An area relative frequency is the proportion of cases for which precipitation occurred at one or more of the gages defining the forecast area.

TABLE 4. Frequency distributions of areal coverage for ten raingages defining forecast area and for four raingages corresponding to the point probability forecasts (n = 222)

Ten raingages			Four raingages		
Areal coverage	Relative frequency	Cumulative relative frequency	Areal coverage	Relative frequency	Cumulative relative frequency
0.00	0.595	0.595	0.00	0.743	0.743
0.10	0.171	0.766	0.25	0.099	0.842
0.20	0.058	0.824	0.50	0.090	0.932
0.30	0.063	0.887	0.75	0.027	0.959
0.40	0.023	0.910	1.00	0.041	1.000
0.50	0.009	0.919			
0.60	0.013	0.932			
0.70	0.032	0.964			
0.80	0.022	0.986			
0.90	0.009	0.995			
1.00	0.005	1.000			

variation and day-night variation in precipitation occurrence during the period of the experiment.

The gage-to-gage variation for individual periods can also be investigated, and the distributions of areal coverage presented in Table 4 indicate that the observations were identical at all ten raingages (precipitation at all ten gages or precipitation at no gages) for 60 per cent of the periods. The comparable figure for the St Louis experiment was 77.7 per cent; as expected, more variability among points was observed at Rapid City than at St Louis. With regard

to day-night differences at Rapid City, the distributions of areal coverage were virtually the same for the two periods.

The point probabilities and the observations, then, both varied considerably from point to point. An ex post evaluation of the forecasts in light of the observations can provide information concerning the extent to which the forecasters were successful in differentiating among the four raingages for which individual point probabilities were assigned. A comparison of the average values of the point probability forecasts (from Table 1) and the corresponding relative frequencies (from Table 3) indicates that with the exception of gage 4, a higher average value of the point probability corresponded to a higher relative frequency. At gage 4, the average probability was reasonably high but the relative frequency of precipitation was lower than at gages 1–3. Some day-night differences existed, and the largest differences between the average values of the point probabilities and the observed relative frequencies occurred at gages 3 and 4 for the day-period forecasts (the forecasts were too high on the average) and at gages 1 and 4 for the night-period forecasts (the forecasts were too low at gage 1 and too high at gage 4).

A more detailed look at the reliability of the point probabilities is provided by a graph of forecast probabilities versus observed relative frequencies. In Fig. 2, such graphs are presented for the entire sample of point probabilities, for the probabilities for gages 1 and 2, and for the probabilities for gages 3 and 4. Overall, the point probabilities tended to be slightly high for low probabilities (i.e. the curve in Fig. 2 is below the  $45^\circ$  line), a result consistent with the results of previous studies (e.g. Hughes, 1965; Sanders, 1973; Winkler and Murphy, 1976). For higher probabilities no systematic bias can be discerned, and in any case the points in Fig. 2 corresponding to high probabilities are based on very few forecasts. When the sample is split into the forecasts for the gages in the hills (3 and 4) and the forecasts for the gages not in the hills (1 and 2), the curves in Fig. 2 indicate that for probabilities larger than 0.20, the probabilities tended to be too high for gages 3 and 4 and too low for gages 1 and 2.

In Fig. 2, observed relative frequencies are plotted as a function of probabilities. An investigation of average probabilities as a function of observations can also provide information about the “goodness” of the forecasts. In Table 5, the average point probability assigned to raingages where precipitation did (did not) occur is presented. For the entire experiment, gages receiving rain were assigned an average probability of 0.376, and gages not receiving rain were assigned an average probability of 0.111. The ratio of these two average probabilities is 3.39, and the corresponding ratios for the day-period and night-period forecasts are 3.21 and 3.72, respectively.<sup>8</sup>

Another type of evaluation of probability forecasts involves scoring rules such as the Brier score (Brier, 1950), which is widely used to evaluate prob-

<sup>8</sup>If the forecasts were perfect, they would always assign probability one to the raingages receiving rain and probability zero to the raingages not receiving rain, in which case the ratio of the probabilities would be infinite.

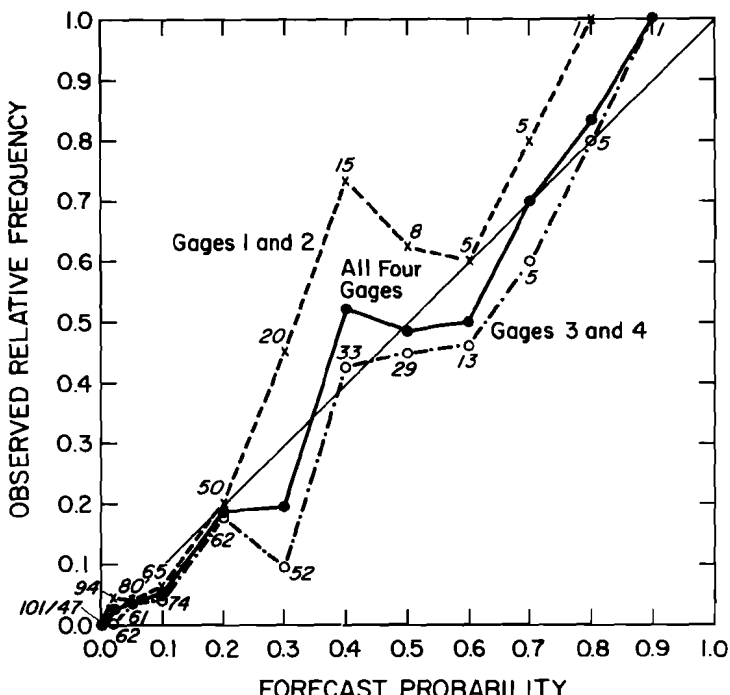


Fig. 2 Forecast probabilities versus observed relative frequencies for the point probability forecasts for all four raingages, for raingages 1 and 2, and for raingages 3 and 4. The number of forecasts is indicated next to each point on the curves for gages 1 and 2 and gages 3 and 4 (for the probability value 0.0, these numbers are 101 and 47, respectively). The number of forecasts for the points on the curve for all four gages is the sum of the corresponding numbers on the other two curves.

ability forecasts in meteorology.<sup>9</sup> For the Rapid City experiment, a quadratic score  $Q$ , which is a linear transformation of the Brier score with a higher score indicating a "better" forecast, was computed as follows for each probability forecast  $p$ :

$$Q(p) = \begin{cases} 1 - (1 - p)^2 & \text{if precipitation,} \\ 1 - p^2 & \text{if no precipitation.} \end{cases}$$

The average quadratic scores for the experimental forecasts are presented in Table 6.

It is difficult to compare scores for different forecasts (e.g. different points for individual point probabilities, area probabilities versus point probabilities) because the scores are sensitive to the distribution of probabilities and to the relative frequency of precipitation. For example, a forecaster can expect to obtain a higher average score for a raingage that seldom receives precipitation than for a raingage that receives precipitation moderately often (e.g. see Glahn and Jorgenson, 1970). In any case, the average scores for the point probabil-

<sup>9</sup>For a general discussion of scoring rules in probability assessment and evaluation, see Winkler and Murphy (1968) or Murphy and Winkler (1970).

TABLE 5. Average point probability assigned to raingages where precipitation did (did not) occur, and ratio of average probabilities at raingages receiving and not receiving precipitation\*

Forecasts	<i>n</i>	$p_R$	$p_{NR}$	$p_R/p_{NR}$
All	222	0.376	0.111	3.39
Day period	112	0.414	0.129	3.21
Night period	110	0.342	0.092	3.72
Forecaster 5	51	0.438	0.125	3.50
Forecaster 7	44	0.415	0.121	3.43
Other forecasters	127	0.337	0.101	3.34

\* $p_R(p_{NR})$  is the average point probability assigned to gages where precipitation did (did not) occur.

ties were higher for gages 1 and 2 than for gages 3 and 4 and were higher for the day-period forecasts than for the night-period forecasts at all gages except gage 3. With regard to individual forecasters, Forecaster 5 received higher than average scores and Forecaster 7 received lower than average scores.

Although it is difficult to interpret average scores per se, a comparison of these scores with scores based on climatological probabilities can provide useful information. Such a comparison can be made using a skill score  $S$ :

$$S = (Q_f - Q_c)/(1 - Q_c),$$

where  $Q_f$  and  $Q_c$  represent the average quadratic scores for the forecast probabilities and the climatological probabilities, respectively. For the Rapid City area, climatological probabilities (for day and night periods by month) were available only for the raingage at the airport (gage 1). Skill scores for  $p_1$  and for  $\bar{p}_f$  evaluated only at gage 1 are presented in Table 6. The positive values of the skill scores for both  $p_1$  and  $\bar{p}_f$  indicate that the forecasters were able to improve upon climatology. Overall, the skill score for  $p_1$  was higher than that for  $\bar{p}_f$ , suggesting that when the forecasters focused their attention upon a single raingage, they were able to formulate somewhat more skillful forecasts.

### b Average Point Probability Forecasts

The forecasters were asked for an average point probability of measurable precipitation for the entire forecast area, and this forecast is denoted by  $\bar{p}_f$ . From Table 1, the average value of  $\bar{p}_f$  was 0.119, and from Table 3, the average relative frequency of precipitation for the ten raingages defining the forecast area was 0.122. The average  $\bar{p}_f$  was slightly higher (lower) than the average relative frequency for the day-period (night-period) forecasts, but these differences were very small. Fig. 3 provides further evidence that the average point probabilities were very reliable; except for high probabilities involving very few forecasts, the graph of  $\bar{p}_f$  versus average relative frequency is very close to the  $45^\circ$  line. With regard to average quadratic scores, the average score for  $\bar{p}_f$  was about the same as the average of the scores for the four individual point probabilities. The average score was higher for night-period than for day-

TABLE 6. Average quadratic scores and skill scores

Forecasts	<i>n</i>	Quadratic scores						Skill scores		
		$p_1$	$p_2$	$p_3$	$p_4$	$(p_1, \dots, p_4)^*$	$\bar{p}_f^†$	$a$	$p_1$	$\bar{p}_f^‡$
All	222	0.934	0.918	0.895	0.917	0.916	0.918	0.826	0.395	0.384
Day period	112	0.946	0.925	0.889	0.920	0.920	0.915	0.808	0.377	0.373
Night period	110	0.923	0.911	0.902	0.913	0.912	0.922	0.845	0.407	0.392
Forecaster 5	51	0.943	0.924	0.904	0.936	0.927	0.930	0.828	0.408	0.461
Forecaster 7	44	0.943	0.911	0.871	0.891	0.904	0.889	0.828	0.363	0.296
Other forecasters	127	0.928	0.919	0.900	0.918	0.916	0.924	0.825	0.408	0.383

\*The average of the scores for  $p_1$ ,  $p_2$ ,  $p_3$ , and  $p_4$ .

†An average score for  $\bar{p}_f$  was computed at each of the ten raingages defining the area, and these scores were then averaged over the ten raingages.

‡Average score for  $\bar{p}_f$  computed for gage 1.

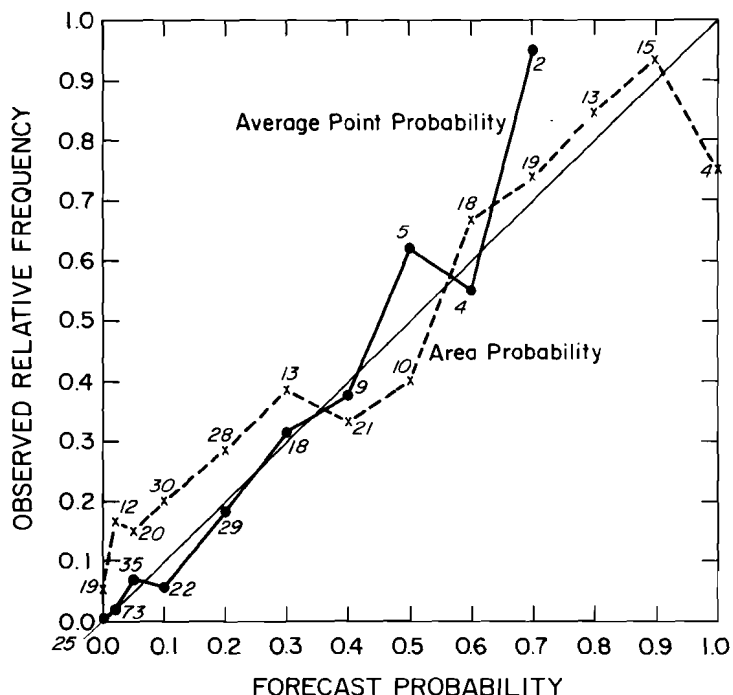


Fig. 3 Forecast probabilities versus observed relative frequencies for the average point probability forecasts and the area probability forecasts. The number of forecasts is indicated next to each point on the two curves.

period forecasts, and Forecaster 5(7) received a higher (lower) than average score.

A different average point probability,  $\bar{p}_c$ , can be calculated by taking the average of the four individual point probabilities for each forecasting occasion. If  $\bar{p}_c$  and  $\bar{p}_f$  referred to the same set of points, then they should be equal, as noted in Winkler and Murphy (1976). However,  $\bar{p}_c$  involved the network of four raingages for which point probabilities were assigned, while  $\bar{p}_f$  involved the larger network of ten raingages defining the forecast area. As can be seen from Table 1, the average value of  $\bar{p}_c$  was somewhat larger than the average value of  $\bar{p}_f$  (0.146, as compared with 0.119). The average relative frequency, however, was also higher for the four-gage network (0.131, as compared with 0.122; see Table 3). It appears that  $\bar{p}_c$  was too high on the average for the day-period forecasts because of the overly high values of  $p_3$  and  $p_4$ .

#### c Area Probability Forecasts

From Table 1, the average value of the area probability forecast, denoted by  $a$ , was 0.356. The comparable relative frequency, the proportion of cases for which precipitation occurred at one or more of the ten raingages defining the forecast area, was 0.405 (Table 3). On the average, then,  $a$  was slightly lower

than the observed relative frequency, and the difference was much larger for the night-period forecasts than for the day-period forecasts. The graph in Fig. 3 suggests that  $a$  tended to be lower than the relative frequency for  $a \leq 0.3$ . However, the overall agreement with the  $45^\circ$  line was quite good, especially when the small number of observations for each  $a$ -value ( $n = 30$  at  $a = 0.10$  was the largest  $n$  for any single  $a$ -value) is taken into consideration. In terms of quadratic scores, the average scores for  $a$  were lower than the average scores for the individual  $p_i$  and for  $\bar{p}_f$ , but this result is probably due to the tendency of  $a$  to be much closer to 0.5 than were the point probabilities. The quadratic score tends to yield higher average scores as the probability forecast deviates more from 0.5. In this regard, note that the average score for  $a$  was better for the night-period forecasts, which were considerably lower on the average than the day-period forecasts.

The consistency of point and area probabilities is also of concern. As indicated in Winkler and Murphy (1976), the area probability should be at least as large as the largest point probability, since precipitation at any point implies precipitation in the area. From Table 1,  $a$  was, on the average, 0.143 higher than  $m$ , the largest of the four point probabilities,<sup>10</sup> and 0.237 higher than  $\bar{p}_f$ . In terms of individual forecasts,  $a < m$  only five times (2.3 per cent of the forecast sets), and these five forecasts were made by only two of the nine forecasters. These results contrast sharply with the results of the St Louis experiment, for which the average difference between  $a$  and  $m$  was negative.

#### **d Expected Areal Coverage Forecasts**

The final forecast made on each occasion was a conditional expected areal coverage forecast. This forecast, denoted by  $e$ , was averaged over those occasions on which precipitation occurred at one or more of the ten gages defining the forecast area, since the forecast was conditional upon the occurrence of precipitation "somewhere in the area." The average value of  $e$  was 0.274, and the average observed conditional areal coverage was 0.301. Thus, the overall correspondence between the average forecast and the average observation was quite close, and these averages were slightly closer for the day-period forecasts (0.281 and 0.300, respectively) than for the night-period forecasts (0.267 and 0.302, respectively). Incidentally, it should be noted that the average observed unconditional areal coverage was only 0.122, which suggests that the forecasters considered the full impact of the conditional nature of the expected areal coverage forecasts appropriately (see footnote 4).

The unconditional expected areal coverage should equal the average point probability,  $\bar{p}_f$  (see Winkler and Murphy, 1976). Therefore, since the conditional expected areal coverage should be greater than or equal to the unconditional expected areal coverage,<sup>11</sup>  $e$  should be greater than or equal to  $\bar{p}_f$ . For

<sup>10</sup>The average value of  $m$  was only 0.008 larger than the average value of  $p_3$ . Thus, the point probability for gage 3 was generally as high as or higher than the other three individual point probabilities.

<sup>11</sup>In fact, the unconditional expected areal coverage should equal the product of the area probability and the conditional expected areal coverage.

the Rapid City experiment  $e - \bar{p}_f$  was 0.055 on the average ( $n = 90$  for  $e$  and  $\bar{p}_f$ ), a result which is consistent in sign with the theoretical relationship between these two types of probabilities.

#### 4 Summary and discussion

The objectives of the St Louis and Rapid City experiments were to investigate the ability of forecasters to formulate point probability forecasts of precipitation occurrence at different points in a forecast area, average point probability forecasts for the area, area probability forecasts, and expected areal coverage forecasts. Rapid City was chosen as the location for the experiment described in this paper because of the existence of a network of raingages and because of significant local effects that were expected to cause variation among points in terms of precipitation occurrence. In this regard, the gage-to-gage variation in precipitation occurrence during the Rapid City experiment far exceeded the variation observed during the St Louis experiment.

The results of the Rapid City experiment indicate that the forecasters differentiated among the points quite often when making point probability forecasts. The point probabilities differed a great deal on the average, and differences within forecast sets were the rule rather than the exception. Thus, the greater point-to-point variability in precipitation occurrence during the Rapid City experiment, as opposed to the St Louis experiment, did enable the forecasters to differentiate among points in terms of precipitation probabilities.

An analysis of the point probability forecasts formulated during the Rapid City experiment indicated that they were reasonably reliable and accurate, with the exception of the forecasts for one particular raingage (gage 4). When the forecasters' lack of experience at making point probability forecasts for different points in the forecast area and the absence of any specific guidance forecasts for these points are taken into account, the reliability and accuracy of the point probability forecasts made during the Rapid City experiment are very encouraging. Presumably, feedback concerning the results and experience over time would lead to improvements in the forecasts for gage 4 as well as in the forecasts for the other gages. In any event, the results indicate that the forecasters at Rapid City were able to differentiate with considerable success among different points in the forecast area in terms of the probability of precipitation.

The relative ability of forecasters to make point and area precipitation probability forecasts in the St Louis and Rapid City experiments was also of interest. At St Louis, the point probabilities, the average point probability, and the expected areal coverage exhibited a high degree of internal consistency, but this consistency may have been facilitated by the lack of variability among points in terms of precipitation occurrence. On the other hand, the area probability tended to be too low (on the average, it was lower than the largest point probability), while the other probability forecasts were quite reliable and accurate in addition to being internally consistent.

At Rapid City, the degree of internal consistency among the different types of forecasts was very high, perhaps surprisingly high in view of the amount of

point-to-point variability in precipitation occurrence. The point probabilities were consistent with the average point probability; the average point probability forecasts were very reliable and accurate; and the expected areal coverage was quite close to the average observed areal coverage. The area probability was slightly lower on the average than the relative frequency of precipitation "in the area," but unlike the St Louis experiment, it was consistent with the point probabilities. The area probability forecast differs enough in nature and complexity from point probability forecasts and average point probability forecasts that the positive results concerning area probability forecasts at Rapid City provide encouraging evidence that forecasters can successfully make this different type of forecast.

The Rapid City experiment suggests that even without training or previous experience, forecasters can differentiate among points in terms of precipitation probabilities with a considerable degree of success and can formulate different types of precipitation probability forecasts, such as area probability forecasts. With some feedback concerning their performance and some additional experience with the different types of precipitation probability forecasts, the performance of the forecasters could be expected to improve still further. An experiment similar to the Rapid City experiment with the inclusion of some mechanism for providing feedback to the forecasters and with an extended experimental period would provide valuable information about the effects of feedback and experience. The results of the Rapid City experiment appear to justify the effort that would be involved in conducting a more extensive experiment, especially in view of the important practical implications of the questions studied in this paper.

In terms of operational forecasting practices, the issuance of different PoP forecasts for different portions of a forecast area seems advisable if a forecaster feels that the probability of precipitation varies appreciably across the forecast area. At locations where a considerable amount of variation exists among points within the forecast area in terms of precipitation occurrence, the failure to recognize this variation when issuing PoP forecasts is misleading and may contribute to skepticism on the part of the public about the "value" of the PoP forecasts. With regard to precipitation probability forecasts other than point probabilities and average point probabilities, the inclusion of these different types of probabilities in forecasts that are issued to the public would necessitate a program to clarify the definitions of different types of probability forecasts<sup>12</sup> and might well represent "overkill" in most forecasting situations. However, certain types of probability forecasts may be valuable to specific users with particular requirements, and some experience at formulating different probability forecasts may provide forecasters with a better understanding of the relationships among the various types of probabilities and may enhance their ability to formulate standard point probability and average point probability forecasts.

<sup>12</sup>Even with respect to current PoP forecasts, a program to educate the public concerning the meaning and use of such forecasts could minimize misinterpretations of the forecasts and could thereby increase their actual value.

## Acknowledgments

We are grateful to the forecasters at the Rapid City wso for their cooperation; to Messrs Don K. Halligan, Meteorologist-in-Charge of the Rapid City wso, and Lawrence A. Hughes, Chief of the Scientific Services Division of the Central Region Headquarters in Kansas City, for assistance that greatly facilitated the conduct of the experiment; to Dr Arnett S. Dennis and Mr James R. Miller, Jr, of the Institute of Atmospheric Sciences (IAS), South Dakota School of Mines and Technology, for assistance in obtaining precipitation observations from selected raingages in the IAS network and for maintaining this network throughout the period of the experiment; and to Dr Nagambal D. Shah and Mr Barry E. Weiss for computational assistance.

---

## References

- BRIER, G.W. 1950. Verification of forecasts expressed in terms of probability. *Mon. Wea. Rev.* **78**: 1-3.
- GLAHN, H.R. and D.L. JORGENSEN. 1970. Climatological aspects of the Brier P-score. *Mon. Wea. Rev.* **98**: 136-41.
- HUGHES, L.A. 1965. *On the probability forecasting of the occurrence of precipitation*. Tech. Note 20-CR-3. Washington, D.C.: U.S. Department of Commerce, Environmental Science Services Administration, Weather Bureau, 36 pp.
- MURPHY, A.H. and R.L. WINKLER. 1970. Scoring rules in probability assessment and evaluation. *Acta Psych.* **34**: 273-86.
- . 1974. Probability forecasts: a survey of National Weather Service forecasters. *Bull. Amer. Meteor. Soc.* **55**: 1449-53.
- SANDERS, F. 1973. Skill in forecasting daily temperature and precipitation: some experimental results. *Bull. Amer. Meteor. Soc.* **54**: 1171-9.
- WINKLER, R.L. and A.H. MURPHY. 1968. "Good" probability assessors. *J. Appl. Meteor.* **7**: 751-8.
- . 1976. Point and area precipitation probability forecasts: some experimental results. *Mon. Wea. Rev.* **104**: 86-95.
-

---

## The Ice Phase and the Evolution of Cloud Droplet Spectra

H.G. Leighton

*Department of Meteorology, McGill University  
Montreal, Quebec*

[Manuscript received 23 September 1976; in revised form 4 January 1977]

---

### ABSTRACT

The effect of the introduction of the ice phase in a cloud droplet growth model is examined. The ice particles are introduced by freezing cloud droplets at rates consistent with observations of natural ice nucleus concentrations. In moderate updrafts the

production of large particles is retarded owing to the glaciation of the cloud. In stronger updrafts where insufficient time is available for precipitation to form by condensation and coalescence, the production of small precipitation particles is increased.

### 1 Introduction

In a previous paper (hereafter referred to as I) Leighton and Rogers (1974) described the changes in cloud droplet spectra as droplets grew by condensation and stochastic coalescence in an ascending parcel of air. One of the main conclusions of that paper was that an appreciable concentration of precipitation-size drops could be produced from a realistic initial droplet distribution containing as many as 900 droplets  $\text{cm}^{-3}$  in the time taken for the parcel to reach the  $-40^\circ\text{C}$  level (less than 15 min). More recently Jonas and Mason (1974) arrived at a similar conclusion on the basis of somewhat different assumptions. The main assumptions in I were (i) that there was saturated adiabatic ascent; (ii) the cloud drops all remained in the parcel; (iii) there was no mixing with ambient air; (iv) no new droplets were nucleated; and (v) there was no ice present. The first three assumptions should be good approximations in the updraft core of a deep convective cloud which would be protected from the environment by a considerable thickness of intervening cloud and where the updraft speeds may be large compared to the terminal fall speeds of drizzle drops. The assumption that there is no further nucleation of cloud droplets is consistent with that of a uniform updraft and should also be valid for accelerating updrafts provided the acceleration is not very large. In cases where the collection rate is so high that the total drop concentration is reduced markedly, nucleation would be important (Young, 1975) but such cases are not considered here. The assumption that has the least justification is the last, namely that the ice phase may be ignored. Since the most rapid development of the droplet spectrum takes place at the highest levels of the parcel ascent it might be expected that allowing for the presence of ice, with the concomitant

absence of ice-ice collection, would seriously retard the spectrum development. On the other hand, since solid hydrometeors will grow more rapidly by sublimation, the overall production of large particles may not be significantly altered.

To describe accurately the development of the ice phase in even as simple a system as an ascending parcel of air is extremely complicated. Ice may nucleate by a number of poorly understood mechanisms and the resulting crystals or frozen droplets will continue to grow by sublimation, by the collection of cloud droplets, and by aggregation with other ice crystals. The growth rates by these different mechanisms are interrelated by their dependence on particle density, shape and temperature, and the ambient vapour pressure.

The most complete treatment of the ice phase in a model of precipitation development is by Young (1974 a, b). He distinguished between a number of different forms of ice particles including crystals of different habits and densities, mixed phase particles, graupel, and snowflakes. Ice formed through contact nucleation and by the activation of deposition nuclei, and the resulting ice particles grew by diffusion and collection. Models with less complex microphysics and correspondingly more simplifying assumptions have been used by Jiusto (1971), Cotton (1972), Danielsen et al. (1972), and Isaac and Douglas (1973) to simulate the formation of ice in updrafts.

The purpose of this work is to determine, by means of a highly simplified model, the seriousness of neglecting the ice phase in I.

## 2 Model description

The present model has as its basis the model of droplet growth by stochastic coalescence and condensation described in I.

To initiate the ice phase cloud droplets are allowed to freeze according to a prescribed freezing rate. From observations of the freezing of water drops formed from bulk precipitation samples collected in Alberta, Isaac (1972) expressed the fraction of the drops of volume  $V$  frozen at a temperature  $T^\circ\text{C}$  by

$$F(T) = 1 - \exp \{-VK(T)\} \quad (1)$$

where,

$$K(T) = C_1 \exp \{-0.576T\}.$$

$C_1$  is of the order of  $7 \times 10^{-2} \text{ cm}^{-3}$  but with some samples having a value of  $C_1$  as much as an order of magnitude smaller. Inherent in the use of the above formula in the present model is the assumption that it is applicable to the freezing of individual drops in a cloud, which may very well not be true. Table 1 shows the fraction of 10 and 100  $\mu\text{m}$  drops frozen at different temperatures. Thus, for instance, if there were 500 droplets  $\text{cm}^{-3}$  of radius 10  $\mu\text{m}$  then, according to Table 1, roughly 0.1 and 15 droplets per litre would be frozen at  $-10^\circ\text{C}$  and  $-20^\circ\text{C}$ , respectively. Although the details of the nucleation mechanism are ignored, the concentrations of ice particles resulting from (1) are in good agreement with deposition nucleus concentrations at  $-10^\circ\text{C}$  (Vali,

TABLE I Fraction of 10 and 100  $\mu\text{m}$  drops frozen

Temp (°C)	Fraction Frozen	
	$r = 10 \mu\text{m}$	$r = 100 \mu\text{m}$
-10	$9.5 \times 10^{-8}$	$9.5 \times 10^{-5}$
-15	$1.7 \times 10^{-6}$	$1.7 \times 10^{-3}$
-20	$3.0 \times 10^{-5}$	$3.0 \times 10^{-2}$
-25	$5.4 \times 10^{-4}$	$4.2 \times 10^{-1}$
-30	$9.5 \times 10^{-3}$	1.0
-35	$1.6 \times 10^{-1}$	
-40	$9.5 \times 10^{-1}$	

1973), and are somewhat higher than the generally accepted ice nucleus concentrations of a few per litre active at -20°C.

The frozen droplets are assumed to remain spherical and to have a density of 1 g  $\text{cm}^{-3}$ . Furthermore, for the sake of simplicity, their fall speeds and collision efficiencies are assumed to be identical to those of the corresponding water droplets. These ice particles grow by sublimation and the collection of water droplets but do not collect other ice particles. Collisional growth is treated stochastically in the same way as the droplet-droplet collisions. Ice-water collisions are assumed to result in spherical ice particles of mass equal to the combined mass of the colliding hydrometeors.

The sublimation growth rate is calculated assuming the simplest form of the diffusional growth equation for spherical ice particles

$$\frac{dr}{dt} = \frac{C}{r}, \quad (2)$$

where  $C$  is proportional to the supersaturation with respect to ice and the well known thermodynamic term (see Fletcher, 1966, p. 267). Provided that the ice concentration is not large, the vapour pressure of the parcel,  $e$ , may safely be taken as the saturation vapour pressure with respect to water,  $e_w$ . The increase in the mass of ice at each time due to sublimation is determined by integrating (2) over the period of one time step (1 s). This mass of water vapour is then reserved for growth by sublimation, which, for reasons explained below, does not take place at every time step. The difference between the change in the ice mixing ratio and the change in the vapour saturation mixing ratio with respect to water is made available for growth of the liquid droplet spectrum by condensation, thus maintaining the total ice and water concentration at the adiabatic value. Eventually, as the ratio of the concentrations of ice to water becomes sufficiently large, this difference becomes negative. That is the sublimation growth rate exceeds the rate at which the adiabatic liquid water content increases. At this stage  $e$  must be less than  $e_w$ . The first estimate of the new value of  $e$  was to take the mean of  $e_i$ , the saturation vapour pressure over ice, and  $e_w$ , weighted by the mass of ice and water respectively:

$$e = \frac{M_i e_i + M_w e_w}{M_i + M_w}. \quad (3)$$

Using this value of  $e$  the change in the ice spectrum is calculated from (2). The droplet spectrum undergoes evaporation, the decrease in mass being such that it compensates for the difference between the increase in the ice concentration and the increase in the adiabatic liquid water content:

$$\left( \frac{dM}{dt} \right)_{\text{evap}} = \left( \frac{dM}{dt} \right)_{\text{subl}} - \left( \frac{dM}{dt} \right)_{\text{ad}}. \quad (4)$$

Thus in the later stages of the ice spectrum development, the sublimation growth rate is determined from (2) and (3), whereas the evaporation rate is determined from (4).

Although the water vapour available for condensation and sublimation is partitioned at each time step, the actual condensation and sublimation calculations take place less frequently. The lower radius limit of the water and ice distributions must correspond to one of the discrete, logarithmically spaced grid points of the radius scale. The spacing between the grid points in turn controls the change necessary in the total mass of the ice or water spectra for a condensation or sublimation event. Since this mass increase will never correspond exactly to the vapour available, as determined by the procedure above, the requirement is imposed that the vapour available and the condensate or sublimate, all averaged over a suitable time interval, must be equal. This is accomplished by requiring condensation or sublimation to take place whenever they would reduce the absolute magnitude of the difference between the total mass of vapour available for each process, summed from the beginning of the parcel ascent, and the accumulated condensate or sublimate. In other words the “reservoirs” of vapour set aside for condensation and sublimation might become negative as long as the absolute value of the contents of each reservoir is the minimum possible.

Freezing takes place immediately after each time that sublimation occurs with the added provision that freezing takes place at least once for every 1°C decrease in parcel temperature. If freezing were allowed to occur significantly less frequently than sublimation, because of the high values of the supersaturation with respect to ice, the lower limit of the ice spectrum might grow rapidly to much larger radii than the corresponding limit of the water spectrum. Then when freezing did occur, the lower limit of the ice spectrum would decrease suddenly to that of the water spectrum, resulting in a discontinuous change in the ice distribution. Because of the relatively large growth rate by sublimation compared to the condensation growth rate, the time interval between sublimation events is shorter than the time interval between condensation events. Thus, although in the upper portion of the ascent the increase in the water content due to condensation tends to be rather discontinuous, the time interval being as much as 90 s, the time interval between sublimation steps is typically less than 5 s.

### 3 Results and discussion

Experiments were run to determine the effect of the ice phase on the hydrometeor distribution in the cloud parcel for a moist atmosphere and two

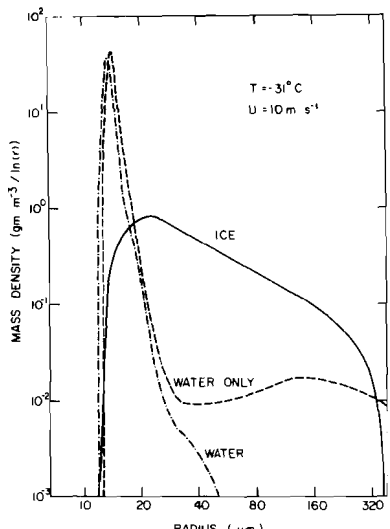


Fig. 1 Mass distributions at the  $-31^{\circ}\text{C}$  level in the  $10 \text{ m s}^{-1}$  updraft; (i) of water droplets from the model without freezing (water only); (ii) of water droplets from the model with freezing (water); and (iii) of frozen droplets (ice).

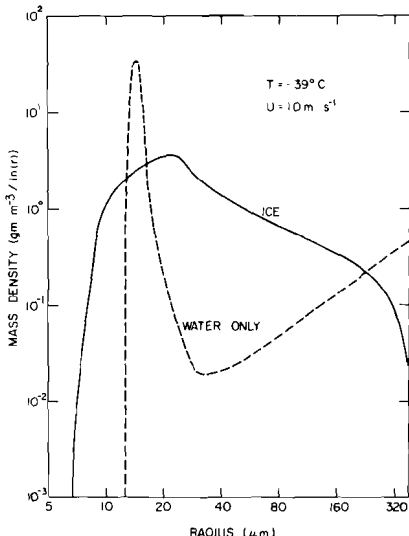


Fig. 2 Same as Fig. 1 at the  $-39^{\circ}\text{C}$  level except that curve (ii) is omitted.

different updraft speeds. Specifically, the cloud is assumed to have a base at 825 mb and  $13.5^{\circ}\text{C}$ . The vertical velocity for the first experiment is taken to be  $10 \text{ m s}^{-1}$ , the parcel starting 800 m above cloud base where the adiabatic liquid water content is  $1.9 \text{ g m}^{-3}$ . The shape of the initial droplet spectrum is a gamma distribution with a concentration of  $900 \text{ droplets cm}^{-3}$ , a mean radius of  $7.8 \mu\text{m}$  and a dispersion of 0.2, resulting in a cloud water concentration equal to the adiabatic liquid water content. The radius of the 100th largest drop  $\text{m}^{-3}$  ( $r_{100}$ ) is sometimes used as a measure of the size of the largest drops in a distribution. The initial distribution defined above has  $r_{100} = 14 \mu\text{m}$ .

Fig. 1 shows the droplet mass distribution after an ascent of 10 min to the  $-31^{\circ}\text{C}$  level for the model without ice, and the droplet and ice spectra for the model with ice, the freezing rate being given by (1). The significant difference between the spectra obtained from the models with and without the presence of ice is the strong enhancement of the number of hydrometeors with radii between 20 and  $200 \mu\text{m}$  in the former compared to the latter. The implication is that growth by sublimation and accretion have more than compensated for the absence of ice-ice coalescence up to this point. Fig. 2 shows the ice spectrum 1.5 min later at  $-39^{\circ}\text{C}$  (by which time freezing is almost complete), and the water spectrum that resulted from the model without ice. At this height the accumulation of particles between 20 and  $150 \mu\text{m}$  radius is still enhanced by the presence of the ice phase. However, whereas the model with ice shows a rapid decrease in the mass distribution of frozen droplets larger than  $150 \mu\text{m}$

TABLE 2 Growth rates of the total ice mass in the  $10 \text{ m s}^{-1}$  updraft

Time (s)	Temp (°C)	Ice Mass ( $\text{g kg}^{-1}$ )	Growth Rate ( $\text{g kg}^{-1} \text{s}^{-1}$ )			
			Freezing	Sublimation	Accretion	Total
300	-8.5	$1.1 \times 10^{-6}$	$5 \times 10^{-8}$	$5 \times 10^{-8}$	$4 \times 10^{-10}$	$1 \times 10^{-7}$
330	-10.6	$6.7 \times 10^{-6}$	$1 \times 10^{-7}$	$3 \times 10^{-7}$	$1 \times 10^{-8}$	$4 \times 10^{-7}$
360	-12.9	$3.3 \times 10^{-5}$	$1 \times 10^{-6}$	$1 \times 10^{-6}$	$2 \times 10^{-7}$	$2 \times 10^{-6}$
390	-14.8	$1.5 \times 10^{-4}$	$2 \times 10^{-6}$	$5 \times 10^{-6}$	$1 \times 10^{-6}$	$8 \times 10^{-6}$
420	-16.9	$6.5 \times 10^{-4}$	$7 \times 10^{-6}$	$2 \times 10^{-5}$	$6 \times 10^{-6}$	$3 \times 10^{-5}$
450	-19.2	$2.7 \times 10^{-3}$	$4 \times 10^{-5}$	$8 \times 10^{-5}$	$3 \times 10^{-5}$	$1 \times 10^{-4}$
480	-21.4	$1.1 \times 10^{-2}$	$1 \times 10^{-4}$	$3 \times 10^{-4}$	$1 \times 10^{-4}$	$6 \times 10^{-4}$
510	-23.8	$4.4 \times 10^{-2}$	$5 \times 10^{-4}$	$1 \times 10^{-3}$	$6 \times 10^{-4}$	$2 \times 10^{-3}$
540	-26.1	$1.8 \times 10^{-1}$	$3 \times 10^{-3}$	$4 \times 10^{-3}$	$2 \times 10^{-3}$	$9 \times 10^{-3}$
570	-28.5	$6.4 \times 10^{-1}$	$9 \times 10^{-3}$	$1 \times 10^{-2}$	$8 \times 10^{-3}$	$3 \times 10^{-2}$
600	-31.0	2.2	$4 \times 10^{-2}$	$4 \times 10^{-2}$	$2 \times 10^{-2}$	$1 \times 10^{-1}$
630	-33.4	5.5	$9 \times 10^{-2}$	$7 \times 10^{-2}$	$3 \times 10^{-2}$	$2 \times 10^{-1}$
660	-36.1	9.4	$9 \times 10^{-2}$	$4 \times 10^{-2}$	$1 \times 10^{-3}$	$1 \times 10^{-1}$

radius, the model without ice shows a continuing increase in the mass distribution beyond this radius. These relatively large liquid drops must have resulted from collisions between particles that would in reality be frozen and hence be unlikely to coalesce. Nevertheless, for the ice distributions of Figs 1 and 2, the values of  $r_{100}$  are  $240 \mu\text{m}$  and  $270 \mu\text{m}$  respectively, indicating the formation of significant numbers of precipitation sized particles by the time the parcel has reached a height of about 7 km above cloud base.

Although it is clear that the largest particles must have grown initially by sublimation and then predominantly by accretion, it is of interest to compare the integrated growth rates of the total ice mass by freezing, sublimation, and accretion. These results are presented in Table 2. The freezing and sublimation growth rates are quite similar over the whole range of the ascent and are significantly larger than the accretional growth rate below the  $-15^\circ\text{C}$  level. Above this level the accretional growth rate becomes comparable to the other two rates, although it is always less than the sublimation growth rate. Accretion is responsible for roughly 20% of the total ice production.

The calculations described above were repeated for an updraft of  $20 \text{ m s}^{-1}$ . The distributions from the models with and without ice are shown in Fig. 3 for the parcel at the  $-39^\circ\text{C}$  level after an ascent of 6 min. Comparison with Fig. 2 shows that the stronger updraft severely inhibits growth by coalescence of water droplets and also retards the formation of ice. In the model without ice no large droplets are produced ( $r_{100} = 17 \mu\text{m}$ ), whereas in the model with ice the corresponding radius is  $90 \mu\text{m}$ . It appears that even in the presence of a strong updraft, ice nucleation may result in hydrometeor spectra with substantially more precipitation-sized particles. Nevertheless, the number of large ice particles is sufficiently small that accretion contributes insignificantly to the total ice concentration present at any height. The production rates of ice by freezing and sublimation are approximately equal.

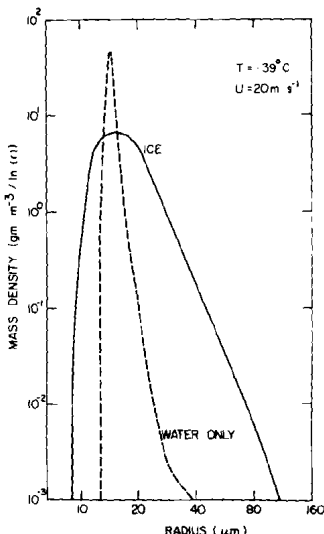


Fig. 3 Same as Fig. 2 for the  $20 \text{ m s}^{-1}$  up-draft.

The question arises to what extent are these results dependent on the assumptions made in introducing the ice phase into the model. Specifically, the sublimation and accretional growth are undoubtedly affected by treating the ice particles as spheres with density equal to the density of water. Also, the procedure for establishing the equilibrium vapour pressure once it falls below the value for water saturation is arbitrary and may seriously influence the final spectra.

Considering the last of these uncertainties first, it is evident that an inconsistency has been introduced. The value of  $(dm/dt)_{\text{evap}}$  found from (4) will not be consistent with the value of  $e$  deduced from (3). To check the extent of this inconsistency, the model calculations for the  $10 \text{ m s}^{-1}$  case are repeated with the droplet evaporation calculated from the value of  $e$  obtained from (3). Thus there is no longer any constraint to maintain a total of condensate plus sublimate equal to the adiabatic liquid water content. This results in ice spectra of similar shape to those of Figs 1 and 2 but of reduced concentration. At the  $-39^\circ\text{C}$  level the total concentration of ice and water is only one-third of the adiabatic value. This low value implies that the estimate chosen for the equilibrium vapour pressure is too low. The actual equilibrium vapour pressure ought to be closer to the saturation value over water in order to reduce the evaporation rate and increase the sublimation rate. Accordingly, the original calculations were repeated, forcing the total of condensate plus sublimate to be equal to the adiabatic liquid water content by adjusting the evaporation rate, but with the equilibrium vapour pressure for the purposes of the sublimation calculation being given by a quite different weighting factor:

$$e = \frac{\sum N_i R_i e_i + \sum N_w R_w e_w}{\sum N_i R_i + \sum N_w R_w},$$

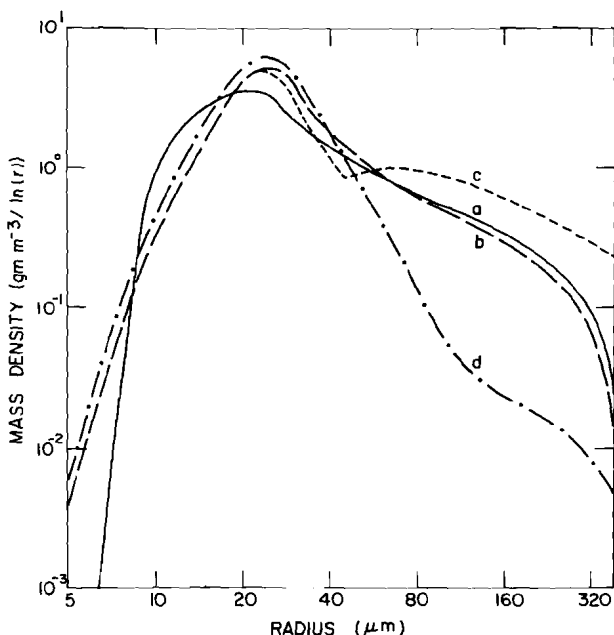


Fig. 4 Sensitivity tests on the model results for the  $10 \text{ m s}^{-1}$  updraft at  $-39^\circ\text{C}$ . a) the same as Fig. 2. b) With the revised scheme for evaluating the saturation ratio as described in the text. c) as b) but with the sublimation rate for particles with  $R > 50 \mu\text{m}$  increased by a factor of three. d) As b) but with the accretion rate of the ice particles reduced by a factor of two.

where  $N_i$  ( $N_w$ ) is the number of ice (water) particles of radius  $R_i$  ( $R_w$ ). The resulting ice spectrum is shown together with the original spectrum in Fig. 4. The small difference between these spectra suggests that the ice spectrum is not sensitive to the supersaturation at the later stages of the ascent where evaporation starts to be important.

The capacitance of small ice crystals will be similar to the capacitance of solid ice spheres of the same mass, and ventilation effects will be unimportant. For crystals with equivalent radius greater than about  $50 \mu\text{m}$  the product of capacitance and ventilation factor is larger than that of water drops of the same mass. Tables of this product by Houghton (1972) suggest that for the solid crystal forms and masses less than  $2 \times 10^{-5} \text{ g}$ , the values are less than a factor of three larger than the capacitance of the equivalent water drop. As a test of the sensitivity of the results to the assumed ice particle capacitance, the model calculations were repeated with sublimation growth rates of ice particles with radius greater than  $50 \mu\text{m}$  increased by a factor of three. The result, plotted in Fig. 4, is an even stronger enhancement of the portion of the spectrum between  $50 \mu\text{m}$  and  $200 \mu\text{m}$ , but still with a rapid fall off in the concentrations at larger radii.

The calculations will be less sensitive to the approximations in the accretional growth of the ice particles due to the off-setting tendencies of the increased sweep-out area and reduced fall speed. Using fall speed and mass-

diameter relationships for lump graupel from Zigmunda and Vali (1972), ratios of sweep-out rates for graupel to water drops with the same mass vary from 50% to 85% for drop radii varying from 60  $\mu\text{m}$  to 400  $\mu\text{m}$ . Recent measurements of collision efficiencies between frozen drops of radii 225  $\mu\text{m}$  and cloud droplets with radii of about 7  $\mu\text{m}$  by Pflaum and Pruppacher (1976) resulted in efficiencies less than one half of those calculated for water drops of the same size. Thus one expects the accretional growth rates in the model to be somewhat overestimated. As a measure of the sensitivity to this uncertainty, the model calculations were repeated again but with the accretional growth rate reduced by a factor of two. The spectrum shows a marked decrease in the mass concentration of the largest ice particles but still exhibits a significant increase in the mass in the radius range 20 to 100  $\mu\text{m}$  compared to the model without ice (Fig. 4).

#### 4 Conclusions

The results of the previous section indicate, that under moist conditions, and moderate updraughts ( $10 \text{ m s}^{-1}$ ), the rapid glaciation of the cloud between  $-30^\circ\text{C}$  and  $-40^\circ\text{C}$  eliminates the high concentrations of particles with radii greater than 200  $\mu\text{m}$  found in I. The presence of small drizzle size particles is enhanced as a result of the favoured growth of ice particles nucleated at warmer temperatures.

In the stronger updraft there is less time available for growth by collection and accretion and so the production of large particles is eliminated. Nevertheless, particles with radii greater than 100  $\mu\text{m}$  are produced in concentrations of about  $100 \text{ m}^{-3}$  at the highest levels in the cloud, in contrast to the results of the model without ice.

The form of the ice spectrum is not sensitive to the saturation ratio at the later stages of the development where the value used in the calculations is most likely to be in error. Rather, it is the sublimational growth in the early stages of the spectrum development followed by accretional growth that determines the concentration of large ice particles. However, it does not appear that these processes are rapid enough to compensate for the absence of self-collection, which must be the dominating growth mechanism in the later stages of the all water model.

#### Acknowledgments

The author is grateful to Dr R.R. Rogers for many helpful discussions. This work was supported by the Atmospheric Environment Service of Canada under Contract Serial No. OSV4-0110.

---

#### References

- COTTON, W.R. 1972. Numerical simulation of precipitation development in supercooled cumuli, Part II. *Mon. Wea. Rev.* **100**: 757-63.  
DANIELSEN, E.F.; R. BLECK; and D.A. MORRIS. 1972. Hail growth by stochastic collection in a cumulus model. *J. Atmos. Sci.* **29**: 135-55.  
ENGLISH, M. 1973. Alberta Hailstorms Part II. Growth of large hail in the storm. *Meteor. Monogr.* **14**: 37-98.

- FLETCHER, N.A. 1966. *The physics of rain-clouds*. Cambridge: Cambridge University Press. 386 pp.
- HOUGHTON, H.G. 1972. Computation of snow crystal growth rates by vapour deposition. *J. de Rech. Atmos.* **VI**: 657–67.
- ISAAC, G.A. 1972. Ice nuclei and convective storms. *Sci. Rept. MW-75*. Montreal: McGill University Stormy Weather Group, 62 pp.
- and R.H. DOUGLAS. 1973. Ice nucleus concentrations at  $-20^{\circ}\text{C}$  during convective storms. *J. Appl. Meteor.* **12**: 1183–90.
- JIUSTO, J.E. 1971. Crystal development and glaciation of a supercooled cloud. *J. de Rech. Atmos.* **V**: 69–85.
- JONAS, P.R. and B.J. MASON. 1974. Evolution of droplet spectra by condensation and coalescence in cumulus clouds. *Quart. J. Roy. Meteor. Soc.* **100**: 286–95.
- LEIGHTON, H.G. and R.R. ROGERS. 1974. Drop-let growth by condensation and coalescence in a strong updraft. *J. Atmos. Sci.* **31**: 271–9.
- PFLAUM, J.C. and H.R. PRUPPACHER. 1976. A wind tunnel investigation of the growth rate and growth mode of ice particles by riming. *Preprints Intern. Conf. on Cloud Physics*, Boulder, pp. 113–16.
- VALI, G. 1973. Remarks on the mechanism of atmospheric ice nucleation. *Proc. 8th Int. Conf. on Nucleation*, Leningrad.
- YOUNG, K.C. 1974a. A numerical simulation of wintertime, orographic precipitation: Part I. Description of model microphysics and numerical techniques. *J. Atmos. Sci.* **31**: 1735–48.
- , 1974b. The conversion of a super-cooled cloud to ice via contact nucleation and direct injection of ice crystals. *Amer. Meteor. Soc. Preprints Conf. on Cloud Physics*, Tucson, pp. 174–9.
- , 1975: The evolution of drop spectra due to condensation, coalescence and breakup. *J. Atmos. Sci.* **32**: 965–73.
- ZIKMUNDA, J. and G. VALI. 1972. Fall patterns and fall velocities of rimed ice crystals. *J. Atmos. Sci.* **29**: 1334–47.

---

## On the Breakdown of the Westerlies

Harald Lejenäs

*Department of Meteorology<sup>1</sup>,  
University of Stockholm,  
Sweden*

[Original manuscript received 4 May 1976; in revised form 25 January 1977]

---

### ABSTRACT

The dynamics of the ultra-long Rossby waves are studied with the aid of a primitive equation numerical model. The investigation is focused on a study of the breakdown of a high-index circulation. Different idealized flow patterns are used as initial conditions and forecasts are made with the numerical model. The influences of oceans and mountains

are studied by incorporating them into the model. The results indicate that barotropic and baroclinic instabilities as well as the structure of the earth's surface are of importance for the development, but the experiments do not clearly indicate which one of these factors is most important.

---

### 1 Introduction

In the present investigation a study of the dynamics of the ultra-long Rossby waves of the atmosphere is performed. Thereby the interplay between various factors such as land and sea distribution, heating from oceans, and non-linear interplay between waves are studied. Such a study can be performed in many ways. It is, however, advisable to concentrate the investigation on a central theme, a certain atmospheric phenomenon to investigate more in detail. One such phenomenon where the factors above are of importance is blocking. Therefore the investigation has been aimed at an attempt to demonstrate the relative importance of the various processes which are expected to play a role in connection with the breakdown of high-index circulation situations.

In spite of the fact that a considerable number of studies of such developments, based on synoptic data, have been undertaken, our understanding of the course of events is far from satisfactory. It hardly seems possible to formulate a general theory.

During the past years considerable attention has been devoted to the stratospheric warming phenomenon which undoubtedly has led to an improved knowledge of what is going on during such events. As regards blocking, on the other hand, comparatively few investigations have been under-

<sup>1</sup>Contribution number 338.

taken, which is surprising in view of the fact that it is accompanied by dramatic alternations between two opposite extreme types of weather.

Blocking is usually considered only in connection with investigations of the motions in the stratosphere and there seems to be a correlation between the occurrence of sudden warmings and blocking action in the troposphere. In case one had strong reasons to believe that blocking were a direct consequence of the development in the stratosphere, this would be a logical approach. In the present investigation we shall, however, adopt the hypothesis that the motions in the troposphere are mainly governed by tropospheric processes. This does obviously not exclude the possibility that stratospheric motion might be strongly dependent on the motions in the troposphere.

We shall briefly recapitulate what is known about the behaviour of the very large-scale flow pattern of the atmosphere. The early investigations of the behaviour of the zonal motion, the development of the long waves, and the subsequent breakdown of the motion and the formation of blocking waves were basically of an observational character (e.g. Garriott, 1904; Berggren, Bolin, and Rossby, 1949; and Rex, 1950).

In conjunction with these studies, attempts were made to advance some theoretical explanations of the phenomenon observed. These may be classified into three types: the barotropic instability theory, the vacillation theory, and the ocean influence theory. Several authors have treated the wave formation and subsequent blocking process as a barotropic instability phenomenon. Thompson (1957), for instance, showed that important features of the mechanism for the initiation and development of blocking are contained in the theory of barotropic flow. A narrow intense jet tends to split into two of lesser intensity, which then rapidly move apart to form the double jet structure. These investigations indicate that the early stages of the formation of blocking to some extent can be simulated with the aid of a two-dimensional theory. However, it is also quite clear that the developments of such events in the atmosphere display a much more complicated pattern. Vacillations were first discovered in the annulus experiments by Hide and Fultz, and later Lorenz (1963) discussed the phenomenon theoretically. Lorenz dealt with the vacillations which appear at a fairly large Taylor number. The question is, however, if the theory explains the phenomenon observed in the annulus experiments, whether those in turn correspond to blocking as observed in the real atmosphere. The temperature difference between the pole and the equator is one of the parameters in this theory. This difference is also a basic parameter in the instability, which thus can be said to be inherent in the vacillation theory. The ocean influence theory, finally, implies that the ocean surface temperature influences blocking. Using a statistical analysis of observed data, Semenov (1960) showed that a close relation exists between the ocean surface temperature and the pressure in a blocking anticyclone. The causal connection between the blocking and the ocean surface temperature may, however, equally well be opposite to the one proposed in this theory.

Later observational studies have illustrated that it is necessary to take into account the three-dimensional structure of atmospheric motion and that

external forces, such as diabatic heating from the oceans and mountains effects, also play an important role. The detailed study of a pronounced cycle of available potential energy (Dec. 1958 – Jan. 1959) carried out by Winston and Kreuger (1961) illustrated this fact rather clearly. These authors found that during this cycle the maxima of the four basic energy quantities, ZAPE (zonal available potential energy), EAPE (eddy available potential energy), ZKE (zonal kinetic energy) and EKE (eddy kinetic energy) occurred in the following order ZAPE, EAPE, ZKE, EKE. The time interval between the first and the last of these maxima was approximately six days. In another observational study of the winter circulation (Jan. 1958), in which also the behaviour of the lower stratosphere was considered in connection with the simultaneous occurrence of blocking and sudden warming, Miyakoda (1963) found similar time variations of the four basic energy components in the troposphere.

Another study of the energy cycle in the lower atmosphere and the occurrence of blocking has been carried out by Murakami and Tomatsu (1965). They pointed out that there are strong energy transformations  $ZAPE \rightarrow EAPE$  and  $EAPE \rightarrow EKE$  for waves with wave numbers 2 and 3 (in January) and that this might be one of the characteristic features of the blocking situation. It was also stressed in this context that blocking is accompanied by a strong northward transfer of sensible heat due to the ultralong waves of wave numbers 2 and 3.

Concerning the definition of the type of motion that is characterized by the breakdown of the zonal westerly motion and the formation of a blocking high, Rex (1950) summarized the most typical features. In spite of the fact that these criteria seem to be rather restrictive, there is no doubt that the development of a flow pattern according to this definition can vary within fairly wide ranges. This has also been pointed out by Miyakoda, Strickler, and Hembree (1970) who stated that part of the difficulties in demonstrating the linkage between the breakdown of the stratospheric vortex and blocking is due to the lack of a clear-cut definition of the blocking process.

The aim of this investigation is thus to contribute to our understanding of the character of the chain of processes that are responsible for the change of the zonal index of the atmospheric motion. For this purpose a numerical forecast experimentation program, based on the ideas we have obtained so far, has been carried out using certain idealized flow patterns as initial fields. By performing such an experimental program in combination with theoretical studies it may be possible to get some indication of how to improve the physical-mathematical models for atmospheric motion.

## 2 Energy changes connected with the breakdown of zonal flow

In this section we shall discuss the information contained in previous studies of the observed behaviour of the four basic energy quantities (ZAPE, EAPE, EKE, and ZKE) when the zonal flow breaks down into cellular flow.

The curves shown in Fig. 1a represent the time variations of these quan-

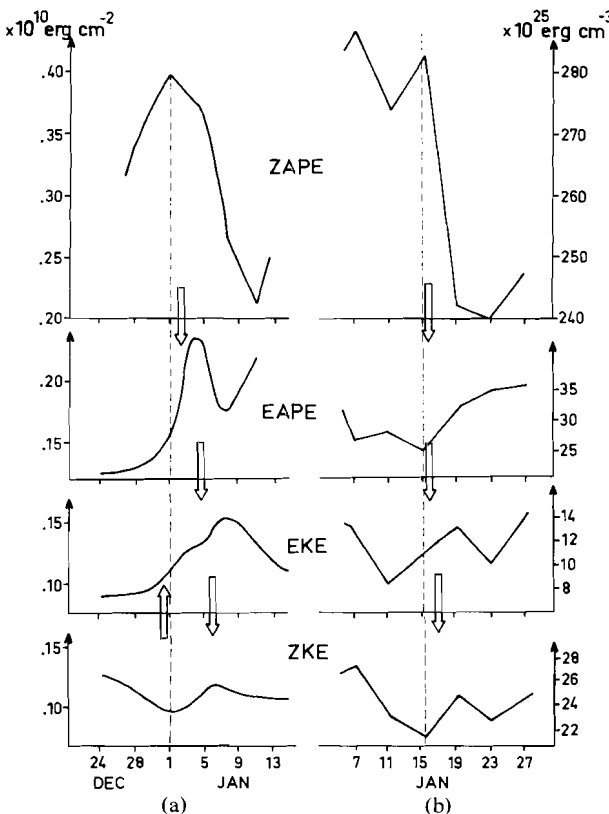


Fig. 1 Time variation of zonal and eddy available potential energy (ZAPE, EAPE) and zonal and eddy kinetic energy (ZKE, EKE) during a blocking situation, as found by Winston and Kreuger, 1961 (1a) and Miyakoda, 1963 (1b). The arrows indicate conversion of energy (Paulin, 1968), and the dash line shows the day of the onset of the blocking.

tities during the period 22 December 1957 to 13 January 1958. They are reconstructed from the investigation by Winston and Kreuger (1961). Since these energy computations show the conditions for the major part of the Northern Hemisphere while the typical developments took place within a certain sector, one cannot expect that the details of these curves contain significant information with regard to our present objective. Furthermore, both in view of the various assumptions introduced in the computations of the energy quantities and the fact that we are interested in the very large-scale processes, it is advisable to consider the basic features of these variations only. They are shown in Fig. 1a. The arrows indicate the direction of the various energy transformations and at which time they attained their maxima as deduced in an investigation by Paulin (1968). The corresponding curves as obtained by Miyakoda (1963) in his study of a similar development which took place in the beginning of Jan. 1958 are shown in Fig. 1b. The comparison of these two cases as shown in the Figs 1a and 1b brings out certain striking

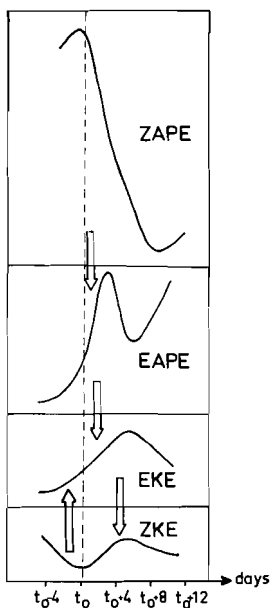


Fig. 2 Idealized picture of the energy changes and energy transformations during a blocking situation. Day  $t = t_o$  is the onset of the blocking.

similarities. It was also pointed out in the second study that similar evolution patterns occur frequently.

We may thus distinguish the following common characteristic features:

- $t \approx t_o - 4$  days      The EKE attains its minimum value while the ZKE decreases. The ZAPE is increasing.
- $t \approx t_o$                   The ZAPE reaches its maximum value, and undergoes thereafter a marked decrease. The ZKE attains its minimum, while the EAPE and the EKE increase.
- $t \approx t_o + 4$  days        The ZAPE undergoes a marked decrease. The EAPE is also decreasing.
- $t \approx t_o + 6$  days        The ZAPE is still decreasing. The ZKE has now its maximum and the EKE reaches its maximum soon afterwards.
- $t \approx t_o + 8$  days        The ZAPE has decreased to the smallest value during the development. The ZKE and the EKE have both undergone a noticeable decrease.

In order to simplify the discussions regarding the processes which may be responsible for the development from a high to a low index circulation, we have taken into account the above-mentioned features and constructed an

idealized picture of the energy changes and energy transformations (c.f. Fig. 2). Concerning the EAPE, there are apparent differences in these two cases. However, we have here chosen the main features in Fig. 1b in view of the likelihood that the variation of this quantity is undoubtedly closely connected with the variation of the generation of eddy potential energy which was evaluated in this case only.

### 3 Theoretical considerations

As a preliminary step in the planning of the numerical simulation of the large-scale motion of the atmosphere during the development from a high-index to a low-index type of circulation, an attempt is made to discuss the interaction between the various processes which may be expected to play an important role in this regard. For this purpose we consider the development from a rather simple initial state, which is characteristic of the basic features of a high-index situation.

We consider a zonal current with both horizontal and vertical shear and assume that it is in geostrophic balance initially. It should be emphasized here that the numerical model utilized for the experiments is a primitive equation model. A description of the model will be given in the next section. A disadvantage of employing a PE model to a geostrophically conditioned initial state is the generation of meridional accelerations initially due to the imbalance. Yet, a strong reason for doing so is the straightforward way the wind and temperature can be related to each other initially. This is important in designing initial conditions that are as simple as possible. Thus we specify the following form of the temperature field in the  $\sigma$ -system ( $\sigma = p/p_s$ ):

$$T(\varphi, \sigma) = \begin{cases} T(\varphi_1, \sigma) & \text{for } \varphi \leq \varphi_1 \\ T(\varphi_1, \sigma) + A(\sigma - \sigma_T) \left\{ \left[ \varphi - \varphi_1 - \frac{D}{2\pi} \sin \frac{2\pi}{D} (\varphi - \varphi_1) \right] \right. \\ \quad \left. + q \left[ \varphi - \varphi_1 - \frac{D}{4\pi} \sin \frac{4\pi}{D} (\varphi - \varphi_1) \right] \right\} & \text{for } \varphi_1 \leq \varphi \leq \varphi_1 + D \\ T(\varphi_1 + D, \sigma) & \text{for } \varphi \geq \varphi_1 + D \end{cases} \quad (1)$$

where

$$T(\varphi_1, \sigma) = T(\varphi_1, 1) \cdot [\max(\sigma, \sigma_T)]^{\gamma R / s}.$$

The corresponding expression for the zonal wind-field is obtained with the aid of the thermal wind equation,

$$U(\varphi, \sigma) = \begin{cases} 0 & \text{for } \varphi \leq \varphi_1 \\ - \frac{RA}{fa} \left\{ \left[ 1 - \cos \frac{2\pi}{D} (\varphi - \varphi_1) \right] + q \left[ 1 - \cos \frac{4\pi}{D} (\varphi - \varphi_1) \right] \right\} \\ \cdot \{1 - \sigma + \sigma_T \ln \sigma\} + \frac{U_s(\varphi) \cdot T(\varphi, \sigma)}{T_s(\varphi)} & \text{for } \varphi_1 \leq \varphi \leq \varphi_1 + D \\ 0 & \text{for } \varphi \geq \varphi_1 + D \end{cases} \quad (2)$$

where  $T_s(\varphi) = T(\varphi, 1)$ ,  $U_s(\varphi) = U(\varphi, 1)$  and  $a$  is the radius of the earth. Note that  $U_{\max}(\sigma) = U(\varphi_1 + D/2, \sigma)$  which will be used later on. The surface wind, which has to be specified, was chosen to be

$$U_s(\varphi) = \frac{U_m}{2} \left\{ \left[ 1 - \cos \frac{2\pi}{D} (\varphi - \varphi_1) \right] + q \left[ 1 - \cos \frac{4\pi}{D} (\varphi - \varphi_1) \right] \right\} \quad (3)$$

The behaviour of the energetics in connection with a blocking situation constitutes the background to the experiments, which means that the conditions summarized in Fig. 2 are to be simulated. The zonal current should thus have the characteristic features of day  $t_o$  in Fig. 2. The zonal available potential energy (ZAPE) should have a large value. The straight zonal current specified by (2) satisfies this condition. Next the EAPE and the EKE should be small. Furthermore they are supposed to increase with time, that is perturbations have to be introduced, and they should amplify during the forecast. Such perturbations can be introduced in different ways. Here small perturbations of a specific kind were introduced into the initial stream function and the surface pressure. According to the energy transformation in Fig. 2 (indicated by arrows) the conversion between EAPE and EKE is small during the initial phase but pronounced later on. Furthermore, a conversion from ZKE to EKE, that is barotropic instability, is observed. These properties are simulated by a zonal current which is barotropically unstable and increasing with height. Perturbations start to amplify due to barotropic instability. The baroclinic instability, inherently due to the vertical wind shear, is initially small, but increases after some time when the wave pattern has amplified. Specifying appropriate values for  $U_m$  and  $q$ , the zonal current given above will have the desirable properties.

The perturbations can now be specified. In order to follow the simple and straightforward approach when deriving the zonal current (2), the perturbations were chosen to be barotropic initially, since a choice of baroclinic perturbations requires a more detailed attention of the balance between wind and mass fields. The perturbation stream function was defined as

$$\psi'(\lambda, \varphi, \sigma, 0) = \begin{cases} = 0 & \text{for } \varphi \leq \varphi_1 \\ = \frac{D}{2\pi} a P_m \left[ 1 - \cos \frac{2\pi}{D} (\varphi - \varphi_1) \right] \\ \cdot \sum_{n=n_1}^N \sin k_n \lambda & \text{for } \varphi_1 \leq \varphi \leq \varphi_1 + D \\ = 0 & \text{for } \varphi \geq \varphi_1 + D \end{cases}$$

where  $k_n$  is the wave number and  $P_m$  is a constant which governs the amplitude of the perturbations. By specifying the index  $n$  it is possible to choose any combination of perturbation wave numbers. The final characteristic feature of Fig. 2 is the large but decreasing value of ZKE at day  $t_o - 4$ . This is expected to be fulfilled automatically due to the fact that there is a strong

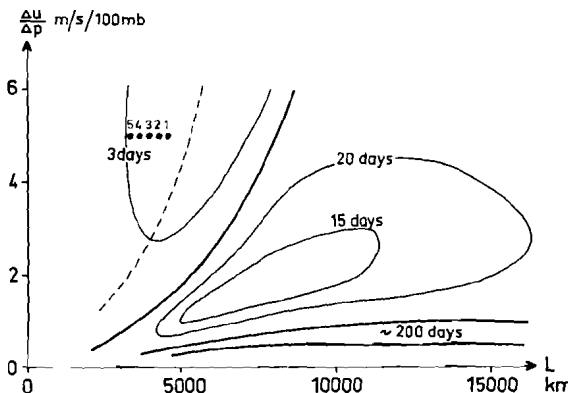


Fig. 3 The growth rate of disturbances in baroclinic flow as a function of wavelength and the vertical shear according to Hirota (1968). The points indicate the stability/instability for wave disturbances in the experiments (see text).

zonal current initially, which decreases with time due to amplifying disturbances.

As was pointed out in the introduction, a general theory for the blocking is not available. We stated, however, that barotropic and baroclinic instabilities are involved. We shall briefly consider these basic instability theories based on linearization to obtain an indication as a qualitative guidance. Hence, we will not go into detailed discussion about this problem in view of the limited applicability of these idealized theories to actual conditions. It is, for instance, known that in a PE model (which we shall make use of), there may be differences in the stability characteristics compared to the quasi-geostrophic studies (c.f. e.g. Gall, 1976). This should be kept in mind when we study Fig. 3 (and later Fig. 4) which shows schematically the growth rate of disturbances in baroclinic flow as a function of the wavelength and the vertical shear. This figure contains the basic features of the diagrams presented by Green (1960) and Hirota (1968) in their studies of baroclinic instability with the aid of quasi-geostrophic frictionless adiabatic linear perturbation theories. As can be seen from this diagram there exist unstable waves for almost all wavelengths and wind shears, but there is only one region in which the growth rates are significant. In that region the time required for *e*-folding the disturbance amplitudes is a few days. The points indicated in Fig. 3 show the amplification rate for wave numbers 1–5 which were used in the first experiment. (See further section 5). Next we shall consider the pure barotropic instability problem. Kuo (1949) applied the instability theory to a zonal (two-dimensional) current and showed that it might be unstable if its absolute vorticity is not a monotonic function of latitude. Many other investigations have also dealt with this problem. In Fig. 4 the instability diagram obtained by Yanai and Nitta (1968) is shown for the kind of wind profile we are using in the present investigation. In the diagram the values that correspond to the chosen

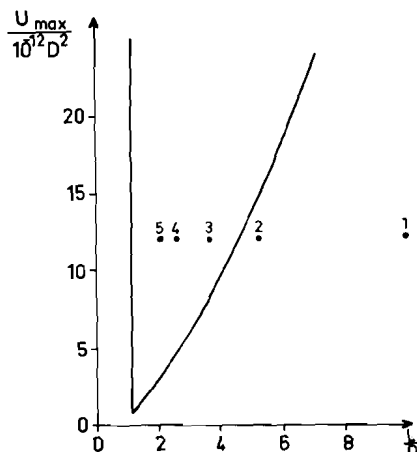


Fig. 4 Instability diagram for symmetric perturbations superimposed on a barotropic zonal current having the horizontal wind profile  $U = 0.5 \times U_{\max} (1 - \cos 2\pi/D_y)$  according to Yanai and Nitta (1968). The points indicate the stability/instability for wave disturbances in the experiments (see text).

values for the width of the current  $D$ , the maximum wind velocity ( $U_{\max}$ ), and the wavelengths of the disturbances which have wave numbers 1, 2, 3, 4, and 5 are also indicated. It should be pointed out here that Jacobs and Wiin-Nielsen (1966) have demonstrated that if the stratification is taken into account, the maximum instability occurs at somewhat longer wavelengths and the growth rate of the unstable disturbances is smaller. They also showed that the energy flow was of the type ZKE → EKE → EAPE when unstable disturbances exist. This uncommon type of energy flow was indeed observed in the beginning of Jan. 1959 at the 100 mb level (c.f. Miyakoda, 1963). Some attempts have been made to clarify the conditions for instability of zonal flows with both vertical and horizontal shear, e.g. Charney and Stern (1962) and Brown (1969). Judging from the results of a "mixed" case which allows for the possibility of the baroclinic and barotropic mechanisms to operate simultaneously, it is apparent that there exist important features which do not show up in either of the two simple field cases.

Besides these instabilities the properties of the earth's surface may be of importance in connection with the breakdown of the zonal motion. To incorporate the effect of the earth's surface, idealized mountains and heating from idealized oceans were introduced into the model. The non-linear interaction between disturbances of different wave numbers is likewise supposed to be important during the initiation of the blocking. This interaction can be simulated by choosing suitable values for  $n$  in the perturbation stream function.

Three experiments were designed to try to separate the importance of mountains, heating from oceans, and the non-linear interplay between the disturbances. In the first one a combination of five waves (wave numbers 1–5) was chosen as perturbations. Mountains and oceans were not introduced. In

the second experiment, heating from an idealized ocean was incorporated into the first experiment, and in the third experiment an idealized mountain was introduced instead of the ocean. Forecasts were then made for five days. The energetics were evaluated every six hours. The result will hopefully give some indication of the importance of the above mentioned parameters.

#### 4 Numerical approach

The numerical model utilized for the experiments is a five-level PE model with sigma as the vertical coordinate. The integration area is hemispheric and Cartesian coordinates in the horizontal are used. The variables on the spherical earth are projected with a polar-stereographic projection on a plane. The prognostic variables are the wind components  $u$  and  $v$ , the potential temperature  $\theta$ , and the surface pressure  $p_s$ . The geopotential  $\phi$  and the vertical velocity  $\dot{\sigma} = d\sigma/dt$  are obtained as diagnostic variables. The model has five equally spaced layers, and  $u$ ,  $v$ ,  $\theta$  and  $\phi$  are obtained at odd levels ( $\sigma = 0.1, 0.3, 0.5, 0.7, 0.9$ ) while  $\dot{\sigma}$  is obtained at even levels. The physical processes considered in the experiments are only surface friction in the boundary layer and horizontal diffusion. The frictional terms are included as the vertical derivative of the torque  $\tau = C_D \rho |V|V$ , where  $C_D$  is the drag coefficient,  $\rho$  the density of dry air and  $V$  the wind velocity at  $\sigma = 0.9$ . A value of  $C_D = 0.002$  was used.

Horizontal diffusion terms were applied to the variables  $u$ ,  $v$  and  $\theta$  in the equations of motion and the thermodynamic equation in order to suppress mainly 2–3Δs waves. At the top and the bottom of the atmosphere  $\dot{\sigma} = 0$ . The model uses an alternating grid, implying that the locations of the variables are different at even and odd time steps. The grid distance was 300 km and the time step 4 min. The model is a simplified version of the one described by Sundqvist (1974).

The analytical expressions for the initial state were derived assuming geostrophic balance. For the experiments the initial state was obtained as follows. From the expression of the zonal current a stream function was derived. The horizontal wind components in the Cartesian grid were then introduced into the model assuming that  $V = k \times \nabla \psi$ , which means that the current is initially non-divergent. Applying the geostrophic conditions at  $\sigma = 1$  we can derive the surface pressure by integration as

$$p_s(\phi) = p_s(\phi_1) \exp \left\{ - \int_{\phi_1}^{\phi} \frac{a}{R} \frac{f(\varphi) U_s(\varphi)}{T_s(\varphi)} d\varphi \right\}$$

where the subscript  $s$  refers to  $\sigma = 1$  (surface);  $p_s(\phi_1)$ , which has to be specified, is the value of the surface pressure at the southernmost latitude of the jet. Finally, it is possible to obtain the potential temperature, knowing the temperature and the surface pressure.

The perturbations were generated in a way similar to the zonal current. The perturbation components of the wind were obtained assuming  $V' = k \times \nabla \psi'$ .

The choice of barotropic perturbations means that  $T' = 0$ . The perturbation field of the surface pressure, finally, was obtained as follows. The expressions for the geostrophic wind components  $u_g$  and  $v_g$  at  $\sigma = 1$  were introduced into the definition of the geostrophic vorticity, which is known. Also knowing the temperature and the Coriolis parameter at each gridpoint, we can compute the surface pressure by a relaxation method. Expressions for the energy quantities and energy transformations are given in the Appendix.

## 5 The experiments

The analytical expressions for the zonal current were given in the previous section. The zonal current in Fig. 4 has a  $1 - \cos 2\pi(\varphi - \varphi_1)/D$  profile, that is, the parameter  $q$  is equal to zero. In the first experiment, weak easterly winds were introduced at the northern and southern boundary of the current, by giving  $q$  the value  $-1/2$ . This was done in order to better reproduce the conditions in the atmosphere. Furthermore it was demonstrated by Fisher and Renner (1971) that the energy conversion rates for  $q \geq 0$  are much smaller than for  $q \leq 0$ . This may also intuitively be realized, since the lateral wind shear for  $q \leq 0$  is more pronounced than for  $q = 0$ . The choice of perturbation wave numbers for the first experiment was based on the observed fact that the distribution of the oceans and the mountains influence wave numbers two and three contain the main part of the energy. Investigating a real blocking situation Berggren et al. (1949) found some interesting features concerning the wavelength of the disturbances. A whole week before the breakdown of the zonal current in the middle of Feb. 1948, migratory cyclones having a wavelength less than 4000 km appeared over the Atlantic. They did not affect the 500 mb current. At the end of that week, disturbances having a wavelength of 4000–5000 km appeared, whereupon the zonal current broke down and a blocking high developed. These observations indicate that waves corresponding to wave numbers 4 and 5 are important, while shorter waves seem to be of minor importance. Thus, wave numbers 1–5 were included in the first experiment. With  $q = -1/2$  the diagram in Fig. 4 will be somewhat modified. An approximate idea of the barotropic instability is, however, obtained from the points given in the figure. Wave numbers 3, 4, and 5 should be barotropically unstable, while 1 and 2 are not. In the same way we get a feeling for the baroclinic instability from Fig. 3, where we notice that all of the wave numbers theoretically have a very similar *e*-folding time, i.e. about 3 days. When utilizing this diagram it is necessary to consider a wavelength  $L$  defined by  $L^{-2} = L_x^{-2} + L_y^{-2}$ , where  $L_x$  is the longitudinal wavelength and  $L_y$  the latitudinal. This implies that also for the ultra-long waves ( $L_x \sim 10,000$  km) the wavelength  $L$  is considerably less than the wavelength for which maximum instability occurs. By this choice of perturbations, the possibility for non-linear interaction among waves was also included.

A five-day experiment was performed with the following parameters:  $\varphi_1 = 42.5^\circ\text{N}$ ,  $q = -1/2$ ,  $D = 20^\circ$ ,  $U_m = 20$  m/s,  $\sigma_T = 0.3$  and  $A = -225$  implying  $U_{\max} = 55$  m/s at  $\sigma = 0.3$ .  $P_m$  in (4) was chosen so that the initial EKE was about 2%

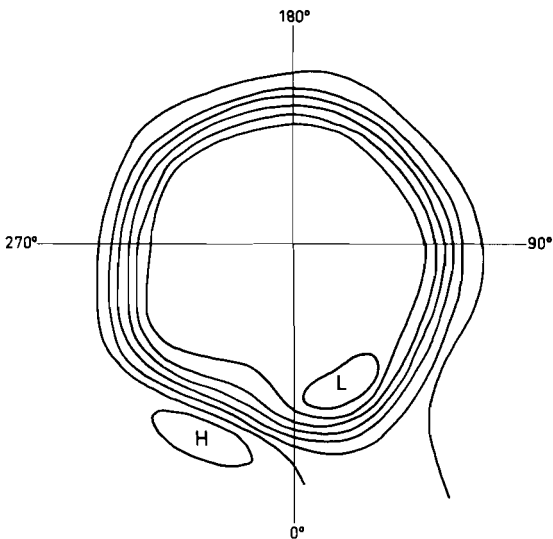


Fig. 5 Initial surface pressure used in the experiments.

of the ZKE, i.e. a relatively weak disturbance. The corresponding surface pressure is shown in Fig. 5. Due to the barotropic perturbations the upper levels have a similar perturbation pattern. Wave number five turned out to be the most unstable one, as five troughs with a slow eastward movement developed. After 3 days one of them deepened more than the others, and after another two days (Fig. 6) a cut-off cyclone ( $L_1$ ) was formed. The energy

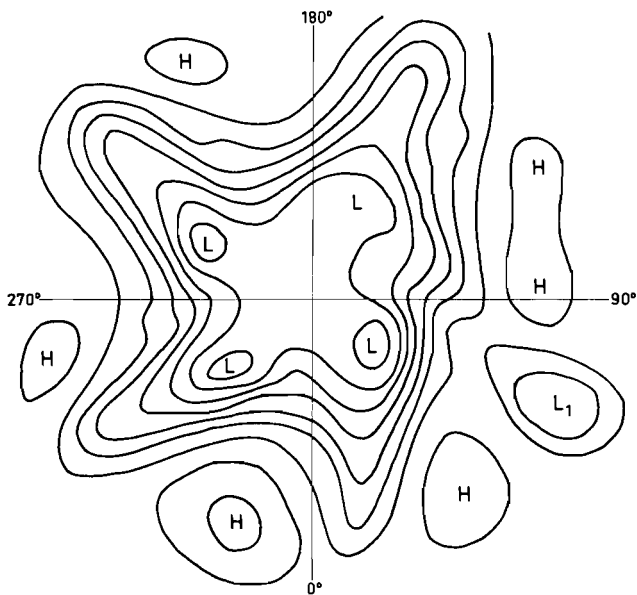


Fig. 6 Experiment I. The 500 mb geopotential height field of a five-day forecast.

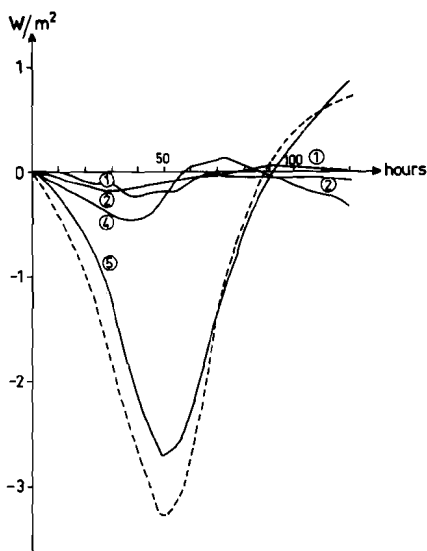


Fig. 7a The conversion term  $C(K_E, K_Z)$  in experiment I. The dashed line is the contribution from all wave numbers, and the full lines are the contributions from individual Fourier components, labelled by wave number.

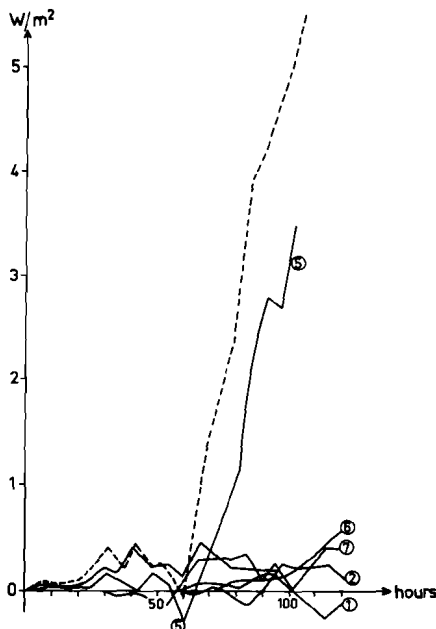


Fig. 7b The conversion term  $C(TPE, K_E)$  in experiment I. The dashed line is the contribution from all wave numbers, and the full lines are the contributions from individual Fourier components, labelled by wave number.

transformations are shown in Fig. 7.  $C(K_E, K_z)$  appears in Fig. 7a. The dashed line shows the contribution from all wave numbers, the full lines represent contributions from specific wave numbers. Fig. 7b shows the same for  $C(TPE, K_E)$ . The development in this experiment shows similarities with the ideal case discussed in section two, such as an initial barotropic instability (Fig. 7a) and an initially weak baroclinic instability increasing after some time (Fig. 7b). Most of the barotropic instability is connected with wave number five and the same is found for the baroclinic instability. A cut-off cyclone is a feature that is typical of blocking. Although the situation after a five-day forecast is far from what characterizes a blocking situation, it is an indication in the right direction.

Next, the effect of the earth's surface was incorporated. In the second experiment the same initial fields were used as in the first experiment. Heating from two idealized oceans was also introduced. The orientation of the oceans is shown in the upper part of Fig. 8. The expression for the ocean surface temperature was assumed to be:

$$T_w(\varphi) = T_w(\varphi_1) - \frac{T_{\text{diff}}}{D_w} \left( \varphi - \varphi_1 - \frac{D_w}{2\pi} \sin \frac{2\pi}{D_w} \varphi \right)$$

where  $T_w$  is the ocean surface temperature and  $T_{\text{diff}}$  the ocean surface tempera-

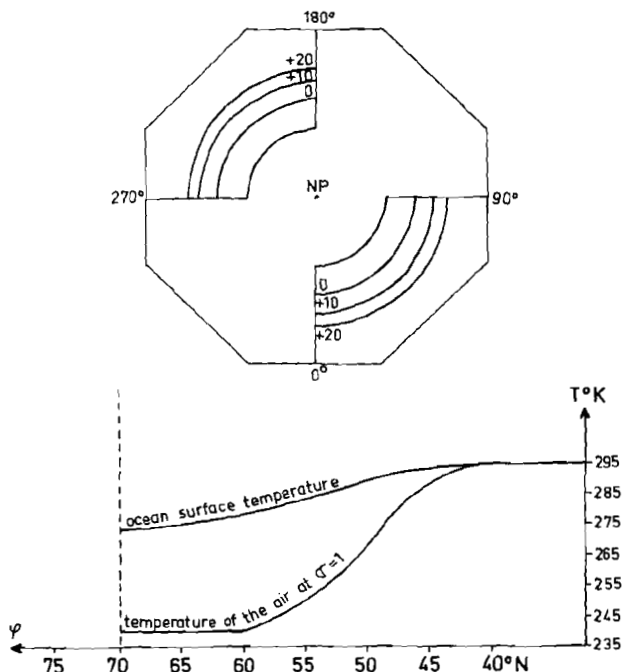


Fig. 8 The location of the oceans in experiment II (upper part), and the latitudinal profile of the ocean surface temperature and the temperature of the air at  $\sigma = 1$  (lower part).

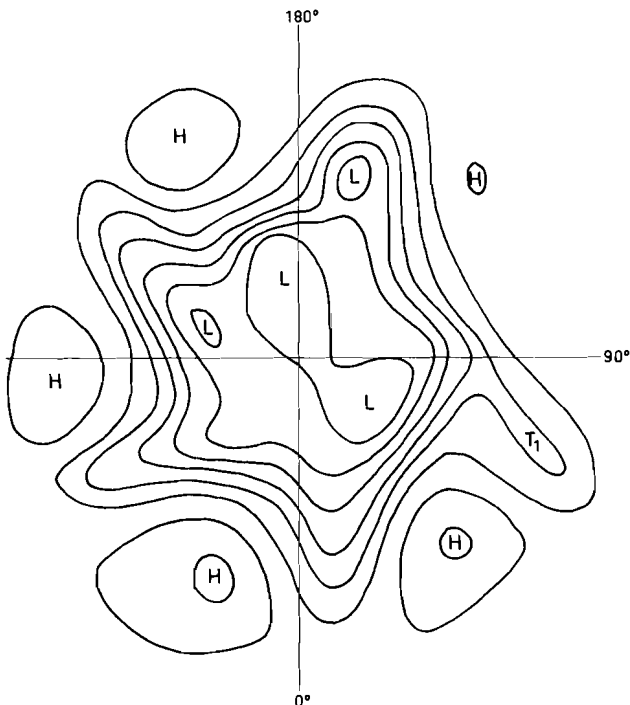


Fig. 9 Experiment II. The 500 mb geopotential height field of a five-day forecast.

ture difference between  $\varphi_1$  and the North Pole. The heating was introduced into the thermodynamic equation according to

$$\frac{d\theta}{dt} = \frac{\theta}{c_p T} \dot{Q}$$

where

$$\dot{Q} = \{c_1 + c_2 \cdot |V_{0.9}| \} \cdot \{T_w - T_a\} \cdot \sigma^r.$$

$T_a$  is the temperature of the air at  $\sigma = 1$ ,  $V_{0.9}$  the wind at  $\sigma = 0.9$ ,  $c_1$  and  $c_2$  constants and  $r$  specifies the vertical distribution of the heating. The following parameters were chosen

$$c_1 = 0.005, c_2 = 0.0015, r = 2, D_w = 50 \pi/180, \varphi_1 = 40 \pi/180.$$

For  $T_w - T_a = 1^\circ$  this yields a heating of  $1^\circ\text{C}$  at  $\sigma = 1$  in a period of 48 hours. The temperature difference  $T_w - T_a$  as a function of latitude at  $t = 0$  can be seen in the lower part of Fig. 8 for  $T_{\text{diff}} = -45$  and  $T_w(\varphi_1) = 295\text{K}$ .  $T_w$  was constant during the forecast, and  $\dot{Q} = 0$  over the continents. North of  $70^\circ\text{N}$  continents were assumed.

A five-day forecast of the 500 mb surface is shown in Fig. 9. Comparison with Fig. 6 shows that the development is weaker than in the second experiment. The cut-off low  $L_1$  in Fig. 6 corresponds to the trough  $T_1$  in Fig. 9. The energy conversion terms  $C(K_E, K_Z)$  and  $C(TPE, K_E)$  are found in Fig. 10a and

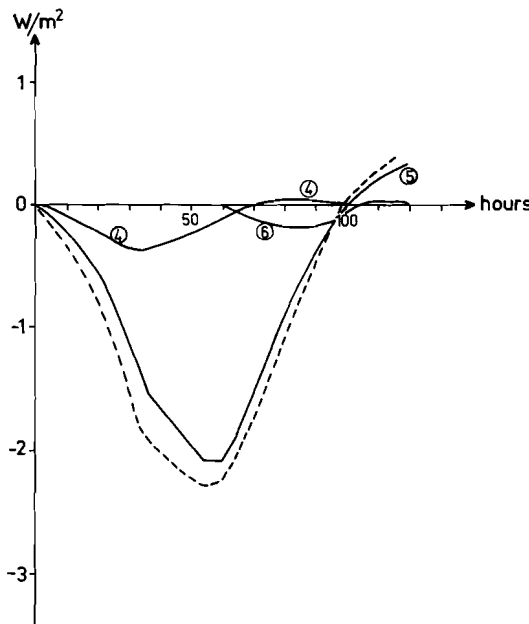


Fig. 10a The conversion term  $C(K_E, K_z)$  in experiment II. The dashed line is the contribution from all wave numbers, and the full lines are the contributions from individual Fourier components, labelled by wave number.

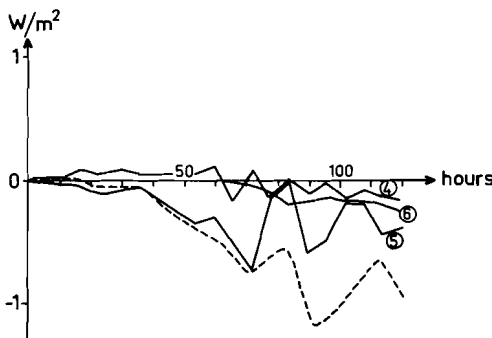


Fig. 10b The conversion term  $C(TPE, K_E)$  in experiment II. The dashed line is the contribution from all wave numbers and the full lines are the contributions from individual Fourier components, labelled by wave number.

10b, respectively. The behaviour of  $C(K_E, K_z)$  is very similar to the result in experiment II. This is true for the total contribution from all wave numbers (dashed line) as well as for the separate wave numbers.

The term  $C(TPE, K_E)$  behaves, however, quite differently. No baroclinic instability is found. Wave number five thus behaves quite differently in experiments I and II (c.f. Fig. 7b and Fig. 10b). The explanation for the behaviour of this conversion term is perhaps to be found in the configuration

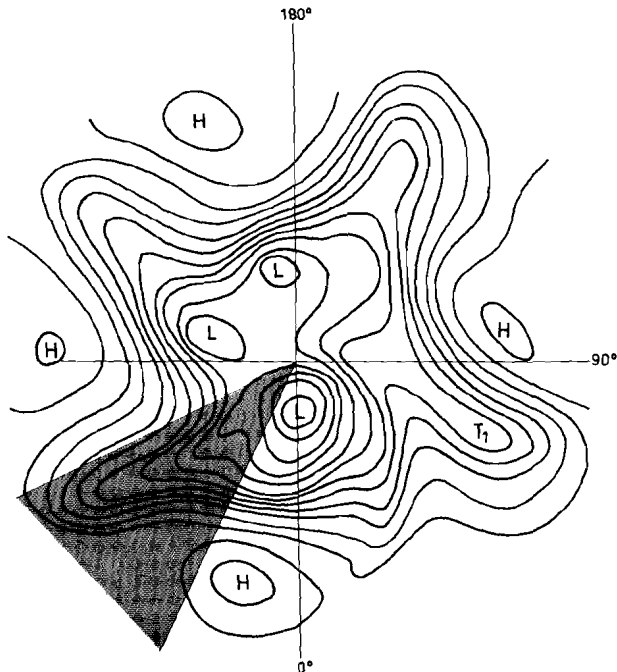


Fig. 11 Experiment III. The 500 mb geopotential height field of a five-day forecast.

of the oceans and the initial disturbances. One important thing may be stated from experiments I and II. Barotropic instability alone obviously cannot produce a breakdown of the zonal motion. Baroclinic instability has to be present, although its presence in experiment I was not sufficient for a clear development towards a blocking.

In the third experiment an idealized mountain was included to study the effect of the orography. The initial fields were the same as in the second experiment. The oceans were not incorporated. A mountain having the dimensions of the Rocky Mountains was introduced in the following way:

$$Z(\lambda, \varphi) = H \sin 8(\lambda + 15) \cdot \delta \quad \text{for } 300^\circ \leq \lambda \leq 322.5^\circ$$

$$Z(\lambda, \varphi) = 0 \quad \text{for } \begin{cases} \lambda \geq 322.5^\circ \\ \lambda \leq 300^\circ \end{cases}$$

where

$$\delta = 1 \quad \text{for } \varphi \leq 45^\circ$$

$$\delta = \sin 2\varphi \quad \text{for } \varphi \geq 45^\circ.$$

The amplitude  $H$  was 2100 m. The definition of the initial fields is based on the fact that the orography is not present. In this experiment, the initial fields had to be established in another way than that described at the end of section 3. This was done by applying the method given by Sundqvist (1975), which implies a solution of the balance equation directly on the sigma surfaces.

The five-day forecast of the 500 mb surface is shown in Fig. 11. The

mountain is indicated by shading. This experiment showed more similarities with blocking than the previous ones. The trough which formed a cut-off low ( $L_1$ ) in experiment two, develops in this experiment to something resembling a real blocking. The trough ( $T_1$  in Fig. 11) is pronounced. A weak ridge is observed north of the trough, and a splitting of the jet is seen. The energy conversion terms are shown in Fig. 12.  $C(K_E, K_Z)$  (Fig. 12a) has a behaviour very similar to that of experiment I and II (Fig. 7a and Fig. 10a).  $C(TPE, K_E)$  on the other hand is quite different. The development due to baroclinic instability is fairly weak during two to three days. After the third day  $C(TPE, K_E)$  increases to values twice as high as in the first experiment (dashed line Fig. 12b). The contribution from the different wave numbers to  $C(TPE, K_E)$  is also seen in Fig. 12b. Wave number five is the most unstable one. Wave number four on the other hand turns out to be baroclinically stable.

The last experiment was the most successful one. The five-day forecast in this case resembles blocking more than in the other experiments. It is obvious that inclusion of orography caused the enhancement of the development. This has also been found in other investigations, e.g. Kikuchi (1971). To illustrate

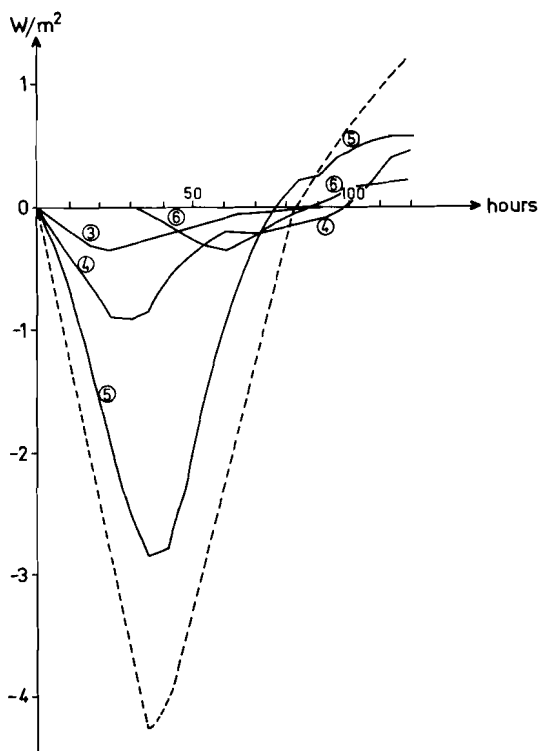


Fig. 12a The conversion term  $C(K_E, K_Z)$  in experiment III. The dashed line is the contribution from all wave numbers, and the full lines are the contributions from individual Fourier components, labelled by wave number.

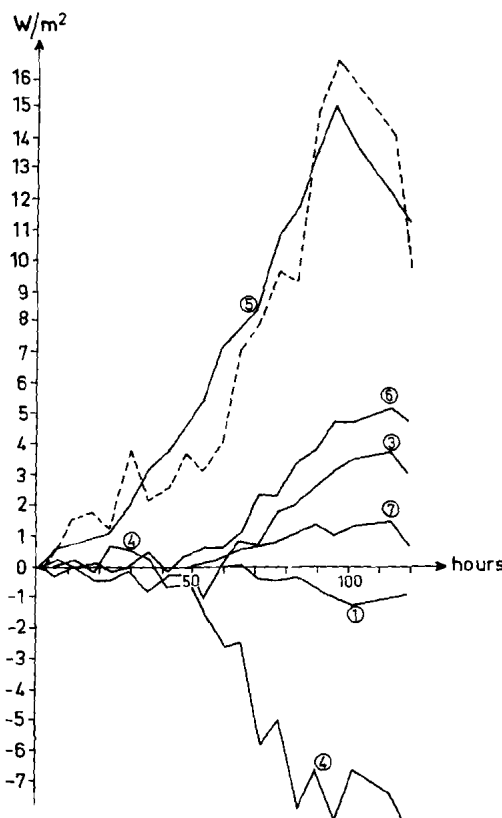


Fig. 12b The conversion term  $C(TPE, K_E)$  in experiment III. The dashed line is the contribution from all wave numbers, and the full lines are the contributions from individual Fourier components, labelled by wave number.

the role played by the two types of forcing, the evolution of the zonal and eddy kinetic energy during the three experiments was depicted. In Fig. 13, showing this, the full lines are from experiment I, the dashed lines from experiment II and the dash-dotted lines from experiment III. As expected, the eddy kinetic energy attains the highest values in experiment III, while experiment II shows the lowest ones. The curves for the zonal kinetic energy show a depletion of the energy of the zonal current, and part of this is fed into the eddy kinetic energy due to barotropic instability. We observe that the amount of zonal kinetic energy in the third experiment between 40 and 80 hours is quite a bit less than in the other two experiments. This indicates that one important reason for the enhanced development is the interaction between the zonal flow and the waves.

A comprehension of the importance of wave-wave interaction is possible to obtain by studying Fig. 14, where the evolution of the wave kinetic energy is plotted (Fig. 14a shows exp. I, Fig. 14b exp. II, and Fig. 14c exp. III). First of

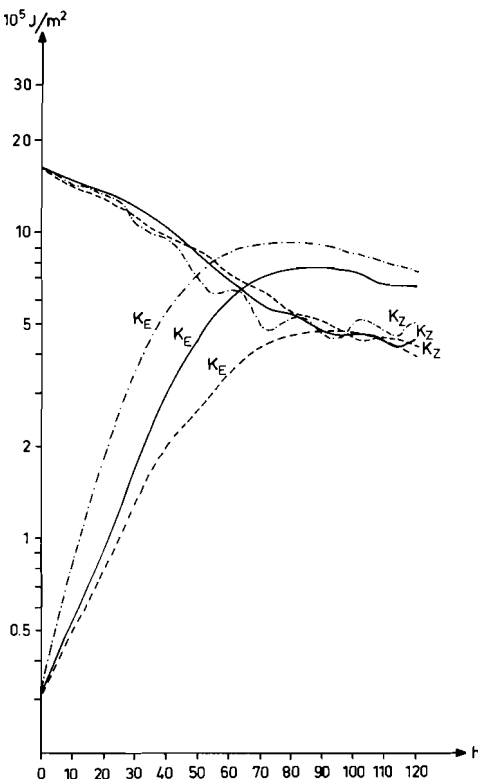


Fig. 13 The evolution of the zonal and eddy kinetic energy during the forecasts. Full lines are from experiment I; dashed lines are from experiment II; and dash-dotted lines are from experiment III.

all it should be stated that these figures reflect energy conversion terms as well as non-linear interactions, so that it is difficult to draw a conclusion. The most outstanding feature is that wave number five behaves very similarly in the three cases. This reflects that there was strong interaction both barotropically and baroclinically between wave number five and the zonal flow. The other wave components do not show the same similarity. One example on non-linear interaction between waves is seen. Wave number six, which was not included in the initial perturbation field, seems to develop due to interaction between wave numbers one and five. In Fig. 14c (exp. III) we notice wave number six already after 30 hours, while in experiment I it appears after 45 hours and in experiment II after 55 hours. The appearance of wave number six is strongly related to the amount of energy in wave numbers one and five.

Another example of wave-wave interaction is seen in wave number four at the end of the five-day forecast in experiment III. The kinetic energy is increasing, but according to Fig. 12 a depletion of energy should take place, since both  $C(TPE, K_E)$  and  $C(K_Z, K_E)$  are negative. The amount of energy fed

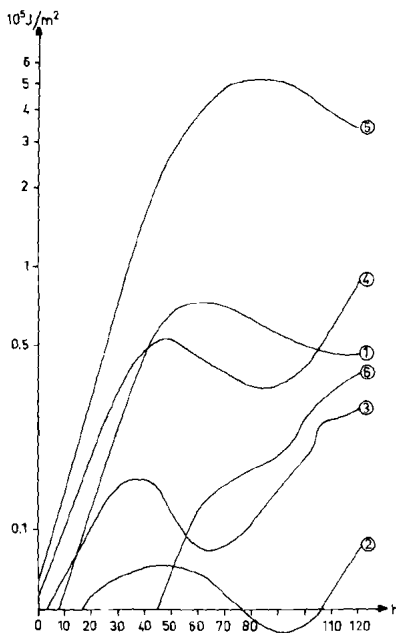


Fig. 14a The evolution of wave kinetic energy during experiment I.

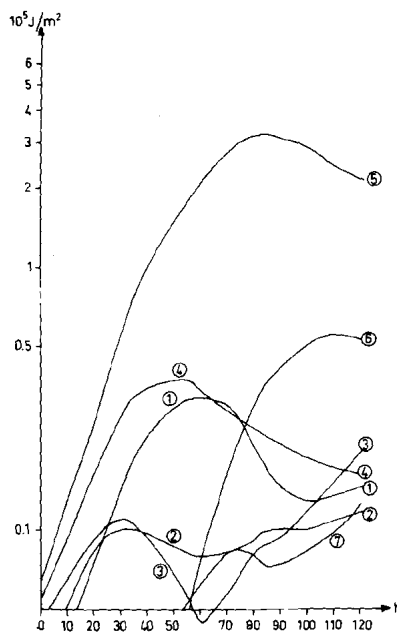


Fig. 14b The evolution of wave kinetic energy during experiment II.

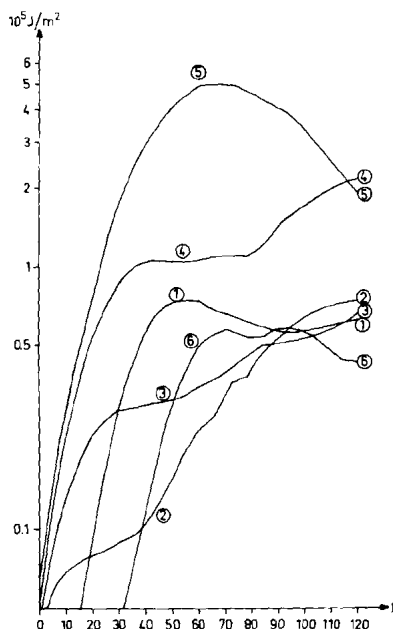


Fig. 14c The evolution of wave kinetic energy during experiment III.

into a wave number due to wave-wave interaction is not large. Still this process goes on, and it may well be partly responsible for the development during the forecasts.

## 6 Concluding discussion

The three experiments described in the last section were designed to clarify the importance of instability processes and different types of forcing in connection with a breakdown of the zonal motion. Experiment I shows that barotropic and baroclinic instability alone is not sufficient for blocking occurrence. Experiment II was aimed at the clarification of the influence of heating from the ocean. It is probable that the result to some extent is dependent on the choice of the idealized ocean. In this second experiment baroclinic instability was absent, and the five-day 500 mb forecast shows the consequences of its absence; for example, the cut-off low is much weaker. The experiments thus show that barotropic instability itself is not capable of initiating a breakdown of the zonal motion. In the third experiment, finally, the importance of the orography was studied. Without hesitation, one can say that the development in this case resembles blocking more than in the other experiments. The reason seems to be an enhanced interaction both barotropically and baroclinically between the waves and the zonal flow. It is also found that non-linear wave interaction may have some importance in this connection.

These experiments were based on an idea established from the observations of the behaviour of the energetics of the real atmosphere during a breakdown of the zonal motion. The experiments may not be considered as conclusive with regard to the possible causes for the breakdown of the zonal motion, but the following may be inferred. The combination of barotropic and baroclinic instability is important. Barotropic instability itself can not cause a blocking. The interaction between the zonal current and waves caused by the distribution of land and oceans (wave numbers 2, 3, and 4) together with barotropic instability and, in a later stage of the development, strong baroclinic instability seem to be the most favourable combination of factors to produce a breakdown of a high-index circulation.

The limited number of experiments can clearly not be considered sufficient for a definite conclusion. Nevertheless it has been possible to draw some conclusions regarding the interplay between various parameters. There are, however, still questions to be answered. One such question is whether the vertical and the horizontal resolution of the numerical model is sufficient. It has been found by Miyakoda et al. (1972) that the long waves of the atmosphere, and especially the ultra-long wave numbers 1 and 2, are forecast in an unsatisfactory way. This was found for the amplitude as well as for the phase speed. They found, however, that a finer horizontal resolution improved the forecast.

The importance of the vertical resolution is less known. Generally we know that more vertical levels yield a better forecast. In connection with a blocking it is observed in the real atmosphere that there is a propagation of energy up

into the stratosphere. Later this energy transport seems to give rise on occasions to a sudden warming in the stratosphere. A question is what would happen if this vertical transport of energy did not take place. It is not quite certain that a numerical model having five vertical levels, the uppermost of them close to 300 mb and 100 mb, can simulate the transport of energy into the stratosphere. It is more plausible that this energy remains in the troposphere.

Possibly a careful study of experiments like the ones here, as well as similar ones, gradually will increase our understanding of the development of atmospheric phenomena.

### Acknowledgments

The author is indebted to Professor Bo Döös who initiated this investigation, and whose ideas about the blocking phenomenon have been pursued in the present paper. Acknowledgment is also made to the National Center for Atmospheric Research, Boulder, Colorado (sponsored by the National Science Foundation) for part of the computer time used in this research.

### Appendix

#### *The Energy Equations*

Making use of the conventional way of visualizing energy budget equations, it is possible to derive the following expressions for the total potential energy (*TPE*), the zonal and eddy kinetic energies ( $K_Z$  and  $K_E$ ).

$$TPE = \frac{1}{2\pi g(\sin \varphi_n - \sin \varphi_s)} \left[ \int_0^{2\pi} \int_{\varphi_s}^{\varphi_n} \int_0^1 c_p \hat{T} p_s \cos \varphi d\lambda d\varphi d\sigma + \int_0^{2\pi} \int_{\varphi_s}^{\varphi_n} \phi_s p_s \cos \varphi d\lambda d\varphi \right] \quad (A1a)$$

$$K_Z = \frac{1}{4\pi g(\sin \varphi_n - \sin \varphi_s)} \int_0^{2\pi} \int_{\varphi_s}^{\varphi_n} \int_0^1 (\hat{u}^2 + \hat{v}^2) p_s \cos \varphi d\lambda d\varphi d\sigma \quad (A1b)$$

$$K_E = \frac{1}{4\pi g(\sin \varphi_n - \sin \varphi_s)} \int_0^{2\pi} \int_{\varphi_s}^{\varphi_n} \int_0^1 (u'^2 + v'^2) p_s \cos \varphi d\lambda d\varphi d\sigma. \quad (A1c)$$

Utilizing the first law of thermodynamics, the equations of motion and the continuity equation it is possible to derive the following conversion terms, where  $C(A, B)$  means conversion of energy from  $A$  to  $B$ :

$$C(K_Z, TPE) = \frac{1}{g(\sin \varphi_n - \sin \varphi_s)} \int_{\varphi_s}^{\varphi_n} \int_0^1 \left[ \bar{p}_s \frac{\hat{v}}{a} \frac{\partial \phi}{\partial \varphi} + R \hat{T} \hat{v} \frac{1}{a} \frac{\partial \bar{p}_s}{\partial \varphi} \right] \cos \varphi d\varphi d\sigma \quad (A2a)$$

$$C(TPE, K_E) = - \frac{1}{g(\sin \varphi_n - \sin \varphi_s)} \int_{\varphi_s}^{\varphi_n} \int_0^1 \left[ \frac{1}{a \cos \varphi} p_s u' \frac{\partial \phi'}{\partial \lambda} + \frac{1}{a} \overline{p_s v' \frac{\partial \phi'}{\partial \varphi}} + \frac{R}{a \cos \varphi} \overline{u' T' \frac{\partial p_s}{\partial \lambda}} + \frac{R}{a} \overline{v' T' \frac{\partial p_s}{\partial \varphi}} \right] \cos \varphi d\varphi d\sigma \quad (\text{A2b})$$

$$C(K_E, K_Z) = \frac{1}{g(\sin \varphi_n - \sin \varphi_s)} \int_{\varphi_s}^{\varphi_n} \int_0^1 \left[ \overline{p_s u' v'} \frac{\cos \varphi}{a} \frac{\partial}{\partial \varphi} \left[ \frac{\hat{u}}{\cos \varphi} \right] + \overline{p_s u' \sigma'} \frac{\partial \hat{u}}{\partial \sigma} + \overline{p_s v' v'} \frac{\partial \hat{v}}{\partial y} + \overline{p_s v' \sigma'} \frac{\partial \hat{v}}{\partial \sigma} \right] \cos \varphi d\varphi d\sigma \quad (\text{A2c})$$

Here the energy budget equations are integrated over a region of mass and given per unit area;  $\varphi_n$  and  $\varphi_s$  are the northern and southern boundaries of the region. We have also made use of the following notations:

$$\bar{\psi} = \frac{1}{2\pi} \int_0^{2\pi} \psi d\lambda \quad \text{zonal average}$$

$$\hat{\psi} = \frac{\overline{p_s \psi}}{\overline{p_s}} \quad \text{pressure weighted zonal average}$$

$$\psi' = \psi - \hat{\psi} \quad \text{deviation from } \hat{\psi}.$$

Note that this implies that  $\overline{p_s \psi'} = 0$ . This is in analogy with what is customarily used in the  $z$ -system. See e.g. Kashara and Washington (1967).

## References

- BERGGREN, R.; B. BOLIN; and C.-G. ROSSBY. 1949. An aerological study of zonal motion, its perturbations and breakdown. *Tellus* **1**, no. 2: 14–37.
- BROWN, J. 1969. A numerical investigation of hydrodynamic instability and energy conversions in the quasi-geostrophic atmosphere. *J. Atmos. Sci.* **26**: 352–75.
- CHARNEY, J.G. and M.E. STERN. 1962. On the stability of internal baroclinic jets in a rotating atmosphere. *J. Atmos. Sci.* **19**: 159–72.
- FISCHER, G. and V. RENNER. 1971. Numerical and analytical studies on the energy conversion in a baroclinic model. *J. Atmos. Sci.* **28**, no. 4: 512–22.
- GARRIOT, E.B. 1904. Long-range forecasts. *U.S. Wea. Bur. Bull.* **35**.
- GALL, R. 1976. A comparison of linear baroclinic instability theory with the eddy statistics of a general circulation model. *J. Atmos. Sci.* **33**, no. 3: 349–73.
- GREEN, J.S.A. 1960. A problem in the baroclinic stability. *Quart. J. Roy. Meteor. Soc.* : 237–51.
- HIROTA, I. 1968. On the dynamics of long and ultra-long waves in a baroclinic zonal current. *J. Meteor. Soc. Japan* **46**: 234–49.
- JACOBS, S.J. and A. WIIN-NIELSEN. 1966. On the stability of a barotropic basic flow in a stratified atmosphere. *J. Atmos. Sci.* **23**: 682–7.
- KASAHARA, A. and W. WASHINGTON. 1967. NCAR global general circulation model of the atmosphere. *Mon. Wea. Rev.* **95**, no. 7: 389–402.
- KIKUCHI, Y. 1971. Influence of mountains and land-sea distribution on blocking action. *J. Meteor. Soc. Japan* **49**, Special Issue: 564–72.
- KUO, H.-L. 1949. Dynamic instability of two-dimensional non-divergent flow in a barotropic atmosphere. *J. Meteor.* **6**: 105–22.
- LORENZ, E.N. 1963. The mechanism of vacillation. *J. Atmos. Sci.* **20**: 448–64.

- MIYAKODA, K. 1963. Some characteristic features of winter circulation in the troposphere and the lower stratosphere. *Univ. of Chicago Tech. Rept No. 14* (Dec.).
- ; F. STRICKLER; and G.D. HEMBREE. 1970. Numerical simulation of the breakdown of a polar-night vortex in the stratosphere. *J. Atmos. Sci.* **27**: 139-54.
- ; G.D. HEMBREE; R.F. STRICKLER; and I. SHULMAN. 1972. Cumulative results of extended forecast experiments. I: Model performance for winter cases. *Mon. Wea. Rev.* **100**, no. 12: 836-54.
- MURAKAMI, T. and K. TOMATSU. 1965. Energy cycle in the lower atmosphere. *J. Meteor. Soc. Japan* **43**, no. 2: 73-89.
- PAULIN, G. 1968. Spectral atmospheric energetics during January 1959. *Publications in Meteor.* no. 91. Montreal: McGill Univ. Arctic Meteorology Research Group.
- REX, D.P. 1950a. Blocking action in the middle troposphere and its effect upon regional climate. I: An aerological study of blocking. *Tellus* **2**: 196-211.
- . 1950b. Blocking action in the middle troposphere and its effect upon regional climate. II: The climatology of blocking action. *Tellus* **2**: 275-301.
- SEmenov, V.G. 1960. The role played by ocean on the formation of blocking anticyclone. *Soviet Meteor.* **5**: no. 2.
- SUNDQVIST, H. 1974. MISU 10-level model. *GARP Publications Series* no. 14 (June): 160-73.
- . 1975. Initialization for models using sigma as the vertical coordinate. *J. Appl. Meteor.* **14**, no. 2: 153-8.
- THOMPSON, P.D. 1957. A heuristic theory of large-scale turbulence and long-period velocity variations in barotropic flow. *Tellus* **9**: 69-91.
- WINSTON, J.S. and A.F. KRUEGER. 1961. Some aspects of a cycle of available potential energy. *Mon. Wea. Rev.* **81**: 307-18.
- YANAI, M. and T. NITTA. 1968. Finite difference approximations for the barotropic instability problem. *J. Meteor. Soc. Japan* **46**: 389-403.

---

## NOTES AND CORRESPONDENCE

---

### CLIMATOLOGICAL STATION HISTORIES

H.B. Kruger

*Atmospheric Environment Service, Downsview*

[Received 31 March 1977]

---

Volume 14, no. 4 of *Atmosphere* contained a note by A.J.W. Catchpole and C. Ponce entitled "Access to Station Histories for Studies of Climatic Change: An Appeal for Improvement" in which they summarized their attempt to survey the history of observational practices in connection with a network of 19 stations recording bright sunshine. Their results were disappointing, and they ended with an appeal for the development of more sensitive station history management practices.

It so happens that a project to upgrade the recording of Canadian station history had been initiated at AES Headquarters a short time prior to the appearance of the issue of *Atmosphere* containing their note.

The note revealed that there was a need to make information available on the extent of the existing AES history resources, and/or how to obtain access to them. Mr G.W.K. MacGregor, the project officer engaged in upgrading the National AES Headquarters station history management system, has prepared a paper entitled "Canadian Climatological Station Histories." This paper will be published as a circular and given the usual distribution by the AES, and will also be available free on request.

Mr MacGregor's paper deals with the following issues:

- a) the nature of the existing AES station history program, and how to obtain access;
- b) the limitations of Canadian climatological station history;
- c) how potential users of station history can help the AES to upgrade the station history program in Canada.

Certain decisions with respect to the development of the new station history program must be made before the end of 1977, so everyone interested in the subject is urged to obtain a copy of the paper, and to communicate their views to us as soon as possible.

Requests for copies should be addressed to:

Atmospheric Environment Service  
Attention ACNN  
4905 Dufferin Street  
Downsview, Ontario, Canada  
M3H 5T4

or telephone (416) 667-4656.

---

## BOOK REVIEWS

---

THE INVISIBLE UNIVERSE. Gerrit L. Verschuur. The English Universities Press Ltd, London; and Springer-Verlag, New York, 1974, 173 pp., paperback, U.S. \$5.90.

This book, subtitled "The Story of Radio Astronomy," is volume 20 in the Heidelberg Science Library. Prof. Verschuur teaches at the University of Colorado in the Department of Astrogeophysics and is also Director of the Fiske Planetarium at Boulder. He writes in a very engaging and entertaining manner. The author is particularly adept at bringing to a lay audience some of the flavour and excitement surrounding the still rapidly evolving field of radio astronomy. Chapter 1 bears the title "Radio Signals From Space and How the Radio Astronomer Picks Them Up." Later, in chapter 18 we read about "How a Radio Astronomer Makes His Observations and Studies the Data." As has now become fashionable, there is not a single equation to be found anywhere in the book. This constraint leads to rather unsatisfying and wordy discussion in places where the essential clarity of a little mathematics would lead to great simplification, or even new insight on the part of the student. An example is the material on the Doppler effect (pp. 62-7). On the other hand, the author's comments on the bandwagon effect—both in the preface and in chapter 9—are delightfully spontaneous and to the point. The more than sixty illustrations in the book are well reproduced and the choice of subject matter is excellent. There is, however, a list of pulsars (Table 3) which is particularly hard to decipher. Someone has achieved another technical breakthrough of questionable merit—reducing 144 lines of computer printout by a factor of sixteen in order to get them all on one page. Some minor errors occur in the text. On page 39, the resolving power of Wild's instrument is incorrectly compared with that of a dish antenna one mile in diameter. Depending on the illumination taper adopted, a dish of 2- or even 3-mile diameter would be required for equivalent resolution. Also, the experiments at Cambridge that led to the discovery of pulsars (p. 115) were carried out at a frequency near 80 MHz, not 100 MHz as stated. Prof. Verschuur adds spice to this informative, well-written book by including a number of anecdotes. The book is up to date and can be highly recommended as an introduction to this very exciting field.

W.K. Klemperer  
Boulder, Colorado

---

## **CALL FOR PAPERS—SYMPORIUM ON THE OCEANOGRAPHY OF THE ST LAWRENCE ESTUARY**

---

Papers are solicited for the coming "Symposium on the oceanography of the St Lawrence Estuary" to be held 12–14 April 1978 at the University of Québec at Rimouski, Rimouski, Québec, Canada. Deadline for receipt of abstracts is 1 November 1977. The topics will include all aspects of oceanography: physics, biology, chemistry, pollution, geology, geochemistry, and fisheries research.

Those who are interested in the Symposium or wish to receive further information on the final program should contact the coordinator: M.I. El-Sabh, Section d'Océanographie, Université du Québec à Rimouski, Rimouski, Qué., Canada.

---

## **APPEL DE COMMUNICATIONS—SYMPORIUM SUR L'OCÉANOGRAPHIE DE L'ESTUAIRE DU ST-LAURENT**

---

Des papiers sont sollicités pour le "Symposium sur l'océanographie de l'estuaire du St-Laurent" qui se tiendra les 12–14 avril 1978 à l'Université du Québec à Rimouski, Rimouski, Qué., Canada. Les résumés définitifs devront être reçus au plus tard le 1er novembre 1977. Le but de ce Symposium est de faire le point des connaissances actuelles de tous les aspects océanographiques de l'Estuaire, soit l'océanographie physique, biologique, géologique, géochimique, la pollution, et les pêches. Ceux qui sont intéressés par le Symposium ou qui veulent avoir d'autres informations sur le programme final devront contacter le coordonnateur: M.I. El-Sabh, Section d'Océanographie, Université du Québec à Rimouski, Rimouski, Qué., Canada.

## INFORMATION FOR AUTHORS

---

**Editorial policy.** *Atmosphere* is a medium for the publication of the results of original research, survey articles, essays and book reviews in all fields of atmospheric science. It is published quarterly by the CMS with the aid of a grant from the Canadian Government. Articles may be in either English or French. Contributors need not be members of the CMS nor need they be Canadian; foreign contributions are welcomed. All contributions will be subject to a critical review before acceptance. Because of space limitations articles should not exceed 16 printed pages and preferably should be shorter.

**Manuscripts** should be submitted to: *Atmosphere*, Dept. of Meteorology, McGill University, 805 Sherbrooke St W., Montreal, Quebec, H3A 2K6. Three copies should be submitted, typewritten with double spacing and wide margins. Heading and sub-headings should be clearly designated. A concise, relevant and substantial abstract is required.

**Tables** should be prepared on separate sheets, each with concise headings.

**Figures** should be provided in the form of three copies of an original which should be retained by the author for later revision if required. A list of legends should be typed separately. Labelling should be made in generous size so that characters after reduction are easy to read. Line drawings should be drafted with India ink at least twice the final size on white paper or tracing cloth. Photographs (halftones) should be glossy prints at least twice the final size.

**Units.** The International System (SI) of metric units is preferred. Units should be abbreviated only if accompanied by numerals, e.g., "10 m," but "several metres."

**Footnotes** to the text should be avoided.

**Literature citations** should be indicated in the text by author and date. The list of references should be arranged alphabetically by author, and chronologically for each author, if necessary.

---

## RENSEIGNEMENTS POUR LES AUTEURS

---

**Politique éditoriale.** *Atmosphère* est un organe de publication de résultats de recherche originale, d'articles sommaires, d'essais et de critiques dans tous les domaines des sciences de l'atmosphère. Il est publié par la SMC à l'aide d'une subvention accordée par le gouvernement canadien. Les articles peuvent être en anglais ou en français. Il n'est pas nécessaire que les auteurs soient membre de la SMC; les contributions étrangères sont les bienvenues. A cause des limitations d'espace les articles ne doivent pas dépasser 16 pages dans le format final. Tout article sera soumis à un critique indépendant avant d'être accepté.

**Les manuscrits** doivent être envoyés à: *Atmosphère*, Dép. de météorologie, L'Université McGill, 805 Sherbrooke O., Montréal, Québec, H3A 2K6. Ils doivent être soumis en trois exemplaires dactylographiés à doubles interlignes avec de larges marges. Les titres et sous-titres doivent être clairement indiqués. Chaque article doit comporter un résumé qui soit concis, pertinent et substantiel.

**Les tableaux** doivent être préparés et présentés séparément accompagnés d'un titre concis et d'un numéro.

**Les graphiques** doivent être présentés en trois copies dont les originaux devraient être conservés par l'auteur au cas où ils seraient nécessaire de les reviser. Une liste des légendes des graphiques doit être dactylographiée séparément. L'étiquetage doit être de grand format de façon à ce qu'il soit facilement lisible après réduction du format. Le traçage des lignes doit s'effectuer au moyen d'encre de chine en doublant, au moins, le format final, le tout sur papier blanc ou sur papier à calquer et identifié adéquatement. Les photographies (demi-teintes) devraient être présentées sur épreuves glacées au double du format final.

**Les unités.** Le Système International (SI) d'unités métriques est préférable. Les unités devraient être abrégées seulement lorsqu'elles sont accompagnées de nombres, ex: "10m," mais "plusieurs mètres."

**Les notes de renvoie** au texte doivent être évitées.

**Les citations littéraires** doivent être indiquées dans le texte selon l'auteur et la date. La liste des références doit être présentée dans l'ordre alphabétique, par auteur et, si nécessaire, dans l'ordre chronologique pour chaque auteur.

The Canadian Meteorological Society came into being on January 1, 1967, replacing the Canadian Branch of the Royal Meteorological Society, which had been established in 1940. The Society exists for the advancement of Meteorology, and membership is open to persons and organizations having an interest in Meteorology. At nine local centres of the Society, meetings are held on subjects of meteorological interest. *Atmosphere* as the scientific journal of the CMS is distributed free to all members. Each spring an annual congress is convened to serve as the National Meteorological Congress.

Correspondence regarding Society affairs should be directed to the Corresponding Secretary, Canadian Meteorological Society, c/o Dept. of Geography, Simon Fraser University, Burnaby 2, B.C.

There are three types of membership – Member, Student Member and Sustaining Member. For 1977 the dues are \$20.00, \$5.00 and \$60.00 (min.), respectively. The annual Institutional subscription rate for *Atmosphere* is \$15.00.

Correspondence relating to CMS membership or to institutional subscriptions should be directed to the University of Toronto Press, Journals Department, 5201 Dufferin St., Downsview, Ontario, Canada, M3H 5T8. Cheques should be made payable to the University of Toronto Press.

---

La Société météorologique du Canada a été fondée le 1<sup>er</sup> janvier 1967, en remplacement de la Division canadienne de la Société royale de météorologie, établie en 1940. Cette société existe pour le progrès de la météorologie et toute personne ou organisation qui s'intéresse à la météorologie peut en faire partie. Aux neuf centres locaux de la Société, on peut y faire des conférences sur divers sujets d'intérêt météorologique. *Atmosphère*, la revue scientifique de la SMC, est distribuée gratuitement à tous les membres. A chaque printemps, la Société organise un congrès qui sert de Congrès national de météorologie.

Toute correspondance concernant les activités de la Société devrait être adressée au Secrétaire-correspondant, Société météorologique du Canada, Département de Géographie, L'Université Simon Fraser, Burnaby 2, B.C.

Il y a trois types de membres: Membre, Membre-étudiant, et Membre de soutien. La cotisation pour 1977 est de \$20.00, \$5.00 et \$60.00 (min.) respectivement. Les institutions peuvent souscrire à *Atmosphère* au coût de \$15.00 par année.

La correspondance concernant les souscriptions à la SMC ou les souscriptions des institutions doit être envoyée aux Presses de l'Université de Toronto, Département des périodiques, 5201 rue Dufferin, Downsview, Ontario, Canada, M3H 5T8. Les chèques doivent être payables aux Presses de l'Université de Toronto.

---

## Council / Conseil d'administration 1976–77

---

*President/Président* – J.E. Hay

*Vice President/Vice-Président* – K.F. Harry

*Past President/Président sortant* –

P.E. Merilees

*Corresponding*

*Secretary/Secrétaire-correspondant* –

R.B. Sagar

*Treasurer/Trésorier* – D.G. Schaefer

*Recording Secretary/Secrétaire d'assemblée* – L.E. Parent

*Councillors-at-large/Conseillers*

– M.G. Ferland, D.B. Fraser,

A.D.J. O'Neill

*Chairmen of Local Centres/Présidents des centres*

*Oceanography Division/Division*

*d'océanographie:*

*Chairman/Président* – D.M. Farmer

*Secretary/Secrétaire* – P.H. LeBlond

*Councillors/Conseillers* – E.P. Jones,

B. Sundby

*Editor/Rédacteur* – J. Derome

*Associate Editors/Rédacteurs adjoints* – C. East, J.B. Gregory, W. Gutzman, P.H. LeBlond,

R. List, C.L. Mateer, G.A. McBean, D.N. McMullen, P.E. Merilees, R.R. Rogers, V.R.

Turner, R.E. Thomson, E.J. Truhlar, E. Vowinkel

*Technical Editor/Editeur technique* – L. Burton

## ATMOSPHERE

---

*Editor/Rédacteur* – J. Derome

*Associate Editors/Rédacteurs adjoints* – C. East, J.B. Gregory, W. Gutzman, P.H. LeBlond,

R. List, C.L. Mateer, G.A. McBean, D.N. McMullen, P.E. Merilees, R.R. Rogers, V.R.

Turner, R.E. Thomson, E.J. Truhlar, E. Vowinkel

*Technical Editor/Editeur technique* – L. Burton

---

*Sustaining Members/Membres de soutien* – Air Canada. – MacLaren Atlantic Ltd.